8-8-2023

Maximum size-density relationships in mixed-species and monospecific stands of the southeastern United States

Maxwell Robert Schrimpf
Mississippi State University, maxwell.schrimpf112@gmail.com

Maximum size-density relationships in mixed-species and monospecific stands of the southeastern United States

By

Maxwell Robert Schrimpf

Approved by:

Adam Polinko (Major Professor)
Austin Himes
Heidi Renninger
Heidi Renninger (Graduate Coordinator)
L. Wes Burger (Dean, College of Forest Resources)

A Thesis
Submitted to the Faculty of
Mississippi State University
in Partial Fulfillment of the Requirements
for the Degree of Master of Science
in Forestry
in the Department of Forestry

Mississippi State, Mississippi

August 2023

Name: Maxwell Robert Schrimpf

Date of Degree: August 8, 2023

Institution: Mississippi State University

Major Field: Forestry

Major Professor: Adam Polinko

Title of Study: Maximum size-density relationships in mixed-species and monospecific stands of the southeastern United States

Pages in Study 82

Candidate for Degree of Master of Science

Maximum size-density relationships (MSDR) are used to quantify differences across sites in the number of trees of a given size and species that can be supported per hectare. These relationships are important to managers who are trying to maximize basal area and wood volume. In my study, I examined MSDR across Alabama, Georgia, Louisiana, and Mississippi using US Forest Service, Forest Inventory and Analysis (FIA) data. I determined the impact of species-specific, specific gravity, functional traits, and environmental factors on MSDR using a quantile regression approach. Overall, I found that climatic factors had the greatest influence on MSDR, and that species shade and drought tolerance were more influential than specific gravity across the southeastern US.

DEDICATION

This thesis is dedicated to Lindy, a good friend and forester who was taken too soon

ACKNOWLEDGEMENTS

I want to acknowledge my professor and mentor, Adam, for his direction and support throughout the project, especially when there were setbacks. His guidance and understanding have led to the success of this project. I wish to thank my committee for their thoughts and contributions to my study, without which this would not have been possible. I also wish to acknowledge my fellow grad students who were invaluable in their help with field work, collaboration of ideas, and their ears during our weekly airing of grievances. I want to recognize and thank my family and my partner, Audra, for their love and support through this process and for believing in me when it was hard to do so myself. I would be remiss to not mention all the foresters I have had the privilege to work with from Ohio, California, Michigan, Mississippi, and the rest of the country who have helped me learn and continued my passion for forestry. Finally, I want to (begrudgingly) acknowledge Escambia Experiment Station, Blackwater River State Forest, and Goethe State Forest for giving me one of the most mentally and physically challenging field assignments I have had.

TABLE OF CONTENTS

LIST OF TABLES

LIST OF FIGURES

CHAPTER I

INTRODUCTION

The development of the stand density index (SDI) by Reineke (1933), put into perspective the relationship between average tree size and overall stand density as a tool for management. Through quantitative research, SDI has been used to guide management based on the theoretical maximum density a stand can support. As a byproduct of its creation, SDI was developed for even-aged, single species stands. Models predicting SDI have been further refined by including tree species, wood density, and climate (Bravo-Oviedo et al., 2018; Chisman and Schumacher, 1940; Ducey et al., 2017; Ducey and Knapp, 2010; Yang et al., 2018). The addition of model parameters has led to more applications of density management being usable in mixed-species stands which traditionally have not had such capabilities (Long and Daniel, 1990). There are several indices relating stand density to an individual tree via allometric relationships and these are useful because they are independent of site quality and stand age (Long, 1985). This allows for comparison across sites. Regulating stands by density becomes important as it has been shown that the average density of stands across the United States (US) has increased while the proportion of low-density stands has decreased (Woodall and Weiskittel, 2021). This change suggests density management will be important as the amount of forestland in the US has remained steady over the last 40 years (Woodall and Weiskittel, 2021).

Objectives

The overarching goal of this thesis is to increase understanding of stand density and the potential factors that would change this relationship. This was done using a quantile regression model of regional US Forest Inventory and Analysis (FIA) stand data on theoretical maximum densities and sensitivities to climate. My study uses FIA data from four southeastern US states to recreate a maximum SDI based on the stand's relative density in single species and simple mixture (of 2-3 species) stands. The first model is a previously developed model intended to test species tolerance with the influence of stress, the other model uses direct climate variables to test external influence. Indicators of climate sensitivity are then added to the first model to enhance the model output. By adding climate variables to the functional traits in an additive fashion, I hope to explore how climate impacts maximum size-density relationships (MSDR).

Through my first model, I tested three hypotheses including:

1. Specific gravity will have a significant impact on MSDR in the southeastern US.
2. Tree species shade tolerance will have a significant impact on MSDR in the southeastern US.
3. Tree species drought tolerance will have a significant impact on MSDR in the southeastern US.

My model building exercise examined the hypothesis that temperature will have a greater effect on MSDR than precipitation in the southeastern US.

CHAPTER II

LITERATURE REVIEW

Stand Density Index

The relationship between stand density and tree size was pioneered by Reineke (1933). He proposed the Stand Density Index (equation 1) based on the relationship between the number of trees per acre and a reference quadratic mean diameter (QMD) (25.4 centimeters, diameter at breast height (DBH)) and assumes a uniform diameter distribution in a monospecific, even-aged stand (Reineke, 1933).

$$\log(N) = -1.605 \log QMD + k \quad (1)$$

Where QMD is 25.4 cm, log(N) is the logarithmic transformation of trees per hectare, and k is a species-specific constant. Reineke's SDI formalizes the principle that a forest stand can support a finite number of trees, of a given size. Reineke (1933) showed that this asymptotic property could be depicted in a linear fashion graphically when both axes were transformed logarithmically (Reineke, 1933). Yoda et al. (1963) later demonstrated a similar concept in agricultural and herbaceous species, showing that this concept was applicable to more than just trees with a self-thinning line of approximately -1.6 (Yoda et al., 1963). With SDI being a guide for density management, Long (1985) connects the practical application of density management by itself to SDI. By showing increasing quadratic mean diameter and trees per hectare (TPH) a

middle ground between single tree and whole stand growth is established. Despite being widely applied, the relationship between stand density and plant size as investigated by Reineke (1933), Yoda et al. (1963), and Long (1985), has been predominantly investigated in even-aged, single cohort, stands of single species, and does not apply in mixed species stands where growth rates differ between species. This somewhat limits its application in most natural stand environments.

Additive Stand Density Index

Since the development of Reineke's SDI, there has been considerable advancement in stand density indices for stands with more complex structure and species composition. For example, an index for measuring stand density was proposed by Long and Daniel (1990), who built off of work by Curtis (1971).

$$ASDI = \sum_{i} N_i \left(\frac{DBH_i}{25}\right)^{1.6} \quad (2)$$

Where ASDI is the additive stand density index, N_i is the number of trees per hectare, and DBH_i is the diameter of the i^{th} tree. The main difference between Reineke's SDI and ASDI was its additive property. They claim that Reineke's index was inappropriate in uneven-aged stands as the stand quadratic mean diameter could not capture the basal area distribution across different diameters. To account for this, they created an additive property where the stand is split into diameter classes and an adjusted SDI is taken for each of these classes (Long and Daniel, 1990). These diameter class means are then summed together to create ASDI. They show that when the diameter distribution of the uneven-aged stand is approximately normal, summed SDI of each class is very close to that of Reineke's stand quadratic mean diameter multiplied by the trees per acre (Long and Daniel, 1990). Recent applications of this research into stand density have used

ASDI to account for greater stand variation in uneven-aged stands. However, even with the trend towards ASDI in the literature as the primary index in more complex stands, it also has limitations. Ducey and Larson (2003), discuss ASDI as compared with Reineke's SDI and whether there is a "correct" density index. They consider three central arguments to ASDI as being a "better" measure of density: historical, geometric, and biological. Overall, they argue that while additivity is useful, that Reineke never intended an additive approach, and these indices should be considered different (Ducey and Larson, 2003). They show that given the different sensitivity of the indices in low diameter stands, other measures of stand density should be considered to determine which is closest to the true maximum. Both stand indices are useful in the right situations, however ASDI is more commonly used for structurally complex stands as it tends to be more accurate in predicting the potential maximum stand density.

Stand Density and Mechanical Stability

The relationship between tree size and stand density is thought to be a function of the available growing space and wood specific gravity (Dean and Baldwin, 1996; Woodall et al., 2005). One of the leading hypotheses about properties of the canopy and its effect on stand density are the physical effects they exert on the stem. It has been shown that there was an inverse relationship between the specific gravity (SG) of wood and the maximum values of stand density index (SDImax) for several species including loblolly pine (*Pinus taeda*) (Dean and Baldwin, 1996). Species with lower specific gravities are thought to need more stem areas to support the same amount of foliage mass per acre than those with high specific gravities (Dean and Baldwin, 1996). Dean and Baldwin (1996) found that, as the average crown ratio (or the proportion of the stem with living crown) increases, SDI decreased while foliage mass increased with increasing SDI. They proposed that species capable of creating higher SDImax would also

have more densely packed leaf area and smaller live crown ratios (Dean and Baldwin, 1996). Mechanically, this translates to the bending stress of the bole and the amount of cross-sectional area (basal area) that is required for a species to support a similar amount of foliage. Think of a tree like a giant lever, taller stems with lower crown ratio (where competition has raised the live crown), are subject to greater bending stress and account for that with increased secondary growth (Dean and Baldwin, 1996). Similarly, Dean (2004) explored the relationship between the behavior of tree crowns and development of the stem. Their main finding was that basal area increment could be modelled based on leaf area and where it accumulated on the stem (Dean, 2004). They explain that, in loblolly pine specifically, fertilization can reduce specific gravity of the wood which is balanced by an increase in the basal area increment to structurally support the additional leaf area load. In addition, their model suggested that to maintain an equal amount of basal area increment through time, stands must either increase their leaf area or raise the average center of leaf area (raising of the crown base) (Dean, 2004). This work was further expanded by work from Woodall et al. (2005) which used the specific gravity concept in SDI to explore mixed species stands by focusing on eight main species (equation 3).

$$E[SDI_{max}] = a_0 + a_1(SG_i) \quad (3)$$

Where $E[SDI_{max}]$ is the expected SDImax of the stand, SG_i is the specific gravity of the i^{th} species, and a_0 and a_1 are estimated coefficients. Their work went further to determine the mean specific gravity of the stand (where SG was averaged) for which maximum ASDI (equation 3) was being calculated (Woodall et al., 2005). Importantly, they found a strong relationship with stand mean specific gravity and the 99^{th} percentile of their observed maximum stand density.

While they still saw over-prediction of SDImax through this method (8%), it was an improvement over previously-used empirical methods (Woodall et al., 2005). Similarly, a non-linear relationship showed that while SG influences stand development, it could not account for the amount of variation in ASDI. In an effort to apply this in mixed-species stands, ASDI was compared to relative densities of several compositions (Ducey and Knapp, 2010). Relative density (RD) was found to not be additive in the same way as ASDI, but was calculated using the required growing space of an individual tree by adapting the tree area ratio (TAR) (equation 4) of Chisman and Schumacher (1940) (Curtis, 1971; Ducey and Knapp, 2010)

$$TAR = c_0 N + c_1 \sum_i DBH_i + c_2 \sum_i (DBH_i)^2 \quad (4)$$

Where TAR is the growing space required for the number of trees in the given stand, N is the number of trees in the stand, $\sum_i DBH_i$ is the sum of diameter of all trees in the stand, $\sum_i (DBH_i)^2$ is the squared sum of diameters of all trees in the stand, and c_0, c_1, and c_2 are estimated coefficients. Curtis (1971) demonstrated a simplified version for the area of a given tree (A_i) using the exponential form in equation 5.

$$A_i = c_1 (\frac{DBH_i}{25})^{1.6} \quad (5)$$

Where c_1 is a species-specific coefficient. Following Ducey and Knapp (2010), the species-specific parameter, c_1 can be related to a tree's SG (equation 6) (Dean and Baldwin, 1996; Woodall et al., 2005)

$$c_1 = b_0 + b_1 SG_i \quad (6)$$

Where SG_i is the specific gravity of the i^{th} species, and b_0 and b_1 are stand-specific coefficients. This creates an RD for stand comparison which is additive like TAR and allows for investigation of different species components in the stand (equation 7), by combining equations 5 and 6 (Ducey and Knapp, 2010).

$$RD = b_0 \sum_i \left(\frac{DBH_i}{25}\right)^{1.6} + b_1 \sum_i SG_i \left(\frac{DBH_i}{25}\right)^{1.6} \quad (7)$$

Where terms are previously defined. In large support of this work, it was found that specific gravity was influential on predicted SDImax based on the amount of hardwood basal area Weiskittel and Kuehne, 2019). This supported hypotheses that higher specific gravities can support greater amounts of leaf area and generally bigger crowns as hardwoods tend to have bigger crown areas (Weiskittel and Kuehne, 2019). Supporting evidence for a positive relationship between specific gravity and leaf area is provided by del Rio et al. (2019) who also found that crown size increased across four species with increasing wood specific gravity. In addition, it was found that in species of higher shade tolerance, crown plasticity increases to accommodate increasing stand densities (del Rio et al., 2019). With many variations of Reineke's principal work in exploring stand density in different ways, the examples above have focused on input data and regression type. Dean et al. (2021) tested Reineke's basic assumptions of the self-thinning line slope (1.6). By inputting foliage density and average live-crown ratio with a random effect in the exponent, they explored a range of exponents (q) based on the relationship between incremental growth of height and volume as a measure of stand density in

Reineke's untransformed equation ($D^q * N$) (Dean et al., 2021). Through this, they computed limits of growing stock which they assume to be parallel with the zone of imminent mortality where self-thinning occurs (Dean et al., 2021). These properties of crown size and density and their relation to stand density support the influence of mechanical strength needed to support the live crown as a likely mechanism explaining the observed relationship between SG and maximum stand density. My study aims to incorporate this connection with climate variables to improve the estimate of maximum stand density.

Stress Tolerance

Tolerance to various stressors also plays an important part in stand density. Species with certain tolerance characteristics are less likely to have decreases in stand density when stressed. Niinemets and Valladares (2006) compared the stress tolerance to shade, drought, and waterlogging for 805 species across North America, Europe, and East Asia. They found that there tends to be trade-offs between shade and drought tolerance (Niinemets and Valladares, 2006). They found the strongest correlation in gymnosperms (Niinemets and Valladares, 2006). It is important to note that species exhibiting polytolerance to these stressors are rare and, in those cases, are not very tolerant to either stressor (Niinemets and Valladares, 2006). Ducey et al., (2017) found predicted maximum SDI in Reineke's SDI and ASDI did not match SDImax when predicted using RD (equation 7) when climate variables (temperature and precipitation) were added. While their study did not use stress tolerance values specifically, the did include climate variables which are related to drought stress. On average, SDI of the study stands was 8% higher when calculated with an additive factor method compared to published SDI guides for the study area (Ducey et al., 2017). A study in northern Spain found that drought tolerance was increasingly important on warmer sites and that drought stress was most likely to reduce stand

densities (Bravo-Oviedo et al., 2018). In the Acadian region of the US, shade tolerance and cold tolerance were some of the key drivers of SDImax in a similar fashion to Reinke's SDI (Andrews et al., (2018).

Comparing Modelling Techniques

Previous studies have compared different modelling techniques for maximum size-density relationships (Andrews et al., 2018; Salas-Eljatib and Weiskittel, 2018). Equation 8 was the top choice of Salas-Eljatib and Weiskittel (2018) as it had limited error in predicting the best and most accurate self-thinning line, although it tended to slightly overpredict maximum stand density (Andrews et al, 2018; Salas-Eljatib and Weiskittel, 2018)

$$SDImax = exp\big((b_0 + k_i) + b_1 * ln(25.4)\big) \quad (8)$$

Using the 95th quantile, it was found that plots with a lower density corresponded with a larger mean tree diameter. A Random Forests variable importance analysis was conducted on the variables and climate scenarios inserted into equation 8 (Andrews et al., 2018). Specific gravity was found to be of high importance in hardwood stands, while time to senescence of leaves was of high importance in conifer stands which aligns with previous work in monocultures (Ducey and Knapp, 2010). Stands dominated by hardwoods were found to have lower SDImax on average, compared to stands dominated by conifers (Andrews et al., 2018). The comparison of models also found dynamic models, which included observations that are remeasured through time, did not significantly improve predictions of self-thinning compared to static models (Salas-Eljatib and Weiskittel, 2018). However, a similar analysis did not show strong correlation of shade tolerance in predicting change of maximum SDI due to species composition, while it did

find support for gradients of SDI across warm, dry sites to cool, wet ones like Ducey et al. (2017) (Weiskittel and Kuehne, 2019).

Climate and Stand Density

It is well known that external factors of climate are just as important in limiting stand density as internal mechanisms. For example, high temperatures, limited moisture availability (Andrews et al. 2020; Salas-Eljatib and Weiskittel 2018), length of the growing season, growing degree days (Anderson-Teixeira et al., 2022; Andrews et al., 2018; Gauli et al., 2022; Kweon and Comeau, 2021), CO_2 concentration (Davis et al., 2022; Duan et al., 2014; Keenan et al., 2014), and vapor pressure deficit (VPD) (Cochard, 2021; Day, 2000; Will et al., 2013) can all limit maximum stand density to levels lower than expected from competition alone. In modelling of SDImax, climate inputs of temperature and precipitation are important. VPD is the difference between the amount of water vapor the air can hold, or saturated vapor pressure, and the actual vapor pressure of the air currently (Hatfield and Prueger, 2015; Lawrence, 2005). The climate variables tested by Andrews et al. (2018) that were important in most of their models included growing season precipitation, annual degree days above 5°C, annual degree days below 0°C, and an interaction involving growing season precipitation and mean temperature of the coldest month (Andrews et al., 2018). Multiple studies found that high stand densities were negatively affected by current year precipitation during periods of limited water (Andrews et al., 2020; Salas-Eljatib and Weiskittel, 2018), and lower density stands are more sensitive to the previous year's precipitation (Andrews et al., 2020). It has been hypothesized that with current climate trends, a broad collection of forest types should expect declining stand densities (Salas-Eljatib and Weiskittel, 2018). While this was demonstrated in already arid systems, it is plausible that similar trends occur in areas where precipitation is not as limited. It was demonstrated in

seedlings, that even with increased carbon dioxide, drought pressures still caused significant mortality through xylem cavitation (Duan et al., 2014). This can become a concern in already arid systems and in systems where moisture could become limiting.

Increasing temperatures are dampening the diurnal effect, changing the length of the growing season, and increasing VPD, all of which may affect maximum stand density (Lee et al., 2021; Meehl et al., 2007). For example, the amount of growing degree days is an important mechanism in SDImax modelling (Andrews et al. 2018; Kweon and Comeau, 2021). Keenen et al. (2014) shows that as the growing season in autumn lengthens, trees take advantage of a longer period to photosynthesize. This could lead to increased volume accumulation on the individual tree level. However, it remains unknown if elevated maximum temperatures in the latter part of the growing season will counter this benefit. In red spruce, it was found that while some trees are more able to adapt to slight changes in VPD, dampening of the diurnal effect could mitigate any increased carbon effect through increased dark respiration this would prevent volume accumulation in trees leading to higher stand densities (Day, 2000). Similarly, chances of hardwood seedling mortality in a forest-grassland transitional area increased with increasing VPD (Will et al., 2013). It is plausible to postulate that seedlings grown in drought-prone areas will select for more drought hardy individuals, however increased VPD, which accompanies areas of drought, may exacerbate the stress by depleting the available soil water more quickly leading to increased mortality (Day, 2000; Will et al., 2013).

CHAPTER III

METHODS, MODELLING, AND MAXIMUM STAND DENSITY

Introduction

Since the development of the stand density index (equation 1) by Reineke (1933), many variations of his equations and similar methods have been tested and compared across different forest types (Reineke, 1933; Salas-Eljatib and Weiskittel, 2018). Reineke's stand density index (RSDI) in its original form relates the number of trees on a per hectare basis to the quadratic mean diameter. It used 25.4 centimeters as a reference QMD yielding a slope of mortality of approximately -1.6 when logarithmically expressed (Ducey and Larson, 2003; Reineke, 1933). It has commonly been applied in single-species stands to relate average growth to density and provide a guide for managers in thinning and harvest operations. Long and Daniel (1990) present an adjusted version of RSDI where the sum of all diameters across the stand were compared to the assumed average of 25.4 centimeters creating the additive stand density index (ASDI). This presents an alternate formulation of the model where individual tree diameters or diameter classes are used and results in ASDI estimates close to that of Reineke's formulation (Ducey and Larson, 2003; Long and Daniel, 1990). Development of measures of relative stand density becomes important as Shaw (2000) developed a proof showing that Long and Daniel (1990)'s method is best in uneven-aged stands as density become more sensitive to the distribution of diameters across a stand (Ducey and Larson, 2003; Shaw, 2000).

While Reineke's SDI was developed for even-aged single species stands, there has been much interest in applying these across uneven-aged, multi-species stands. However, development of additive, quantile methods have allowed greater application of SDI in mixed species and uneven-aged stands. By attempting to account for stem biomechanics, environmental and climatic stressors, and changes of maximum stocking based on site, it is easier to apply these techniques in complex stand structures. While there has been much work using these methods across the Lake States (Ducey et al., 2017; Ducey and Knapp, 2010; Woodall et al., 2005), the Acadian region (Andrews et al., 2018; Weiskittel and Kuehne, 2019), and the Pacific Northwest (Curtis, 1971; Reineke, 1933), there is a literature gap for the southeastern US that does not specifically focus on commercial species (Burkhart and Yang, 2022; Dean and Baldwin, 1996). In an attempt to bridge this gap, my analysis explores the relationship between SG, climate, shade and drought tolerance, and size/density relationships of southeastern forests using data from the US Forest Service, Forest Inventory and Analysis. Specifically, my hypotheses were:

1. Specific gravity will have a significant impact on maximum size-density relationships (MSDR) in the southeastern US.
2. Tree species shade tolerance will have a significant impact on MSDR in the southeastern US.
3. Tree species drought tolerance will have a significant impact on MSDR in the southeastern US.
4. Temperature will have a greater effect on MSDR than precipitation in the southeastern US.

Methods

Data Aggregation

Study Area

I focused on forest data from the states of Mississippi, Alabama, Georgia, and Louisiana, US. Making up a large part of the southeastern US, their total land area combined is 55,076,874 hectares. Of this, 32,374,851 hectares (59%) is forested with a majority of it being privately owned (*Alabama Forestry Commission*, 2021; *Georgia Forestry Commission*, 2020; "Louisiana Department of Agriculture and Forestry," n.d.; *Mississippi Forestry Commission*, 2020). The study area comprises many different soil types ranging from upland, well-drained sites to floodplains and terraces that are very poorly drained. A noticeable shift in soil types occurs when crossing the Mississippi River from east to west, this defines the change from the southern coastal plain to the western coastal plain of Louisiana. On the ends of the range, Georgia and Alabama share the foothills of the Appalachian plateau and the Piedmont which transition from upland, well drained sites into red-clay loams to the Gulf Coast marshes of Louisiana which are very deep, have heavy clay and are very poorly drained (Hancock et al., 2014; Kushla and Oldham, 2020; Mitchell, Jr., 2008; Weindorf, 2008). The climate of the southeastern US is characterized by high humidity and a subtropical pattern. Most of the precipitation occurs during the fall, winter, and spring with less precipitation during the summer months (McNulty and Gavazzi, 2022). The temperature and moisture regimes of this region are influenced by the El Nino-Southern and North Atlantic Oscillations and further impacted by tropical storms and hurricanes on a regular basis (McNulty and Gavazzi, 2022).

Forest Inventory and Analysis

The FIA inventory protocol established a series of three subplots that are clustered around a central subplot at designated angles (Bechtold and Patterson, 2015). One cluster plot includes all four subplots. Each FIA cluster plot represents 2428 ha (6000 ac). By counting each cluster plot as a single "stand" observation, this eased the need for subdivision of the subplots. For more information on FIA protocol, refer to Bechtold and Patterson (2015). Plots are measured on a rotation of 5-7 years depending on the state.

Data were downloaded from the FIA datamart (US Department of Agriculture, Forest Service, Northern Research Station, 2023, Accessed October 2021) and imported using the rFIA package (Stanke et al., 2020). All sampling years of FIA data were used in this study. Since FIA data are taken across both public and private lands to create a national inventory, the exact plot center locations are not available in the public access data. A random dithering is applied as a measure of landowner privacy and to protect the integrity of the FIA plot (Lister et al., 2005; USDA Forest Service, 2022). Prior to 2002, the plot locations as recorded by the forester were within 1.6 km of the actual plot center. Currently, plots are protected through slight shifting of the coordinates and sometimes a "swap" where plot data is swapped within a county with plots of like demographics (Coulston et al., 2006; Lister et al., 2005).

Climate NA and Stress Tolerance Data

Historical climate data were acquired using Climate NA by FIA plot location (Wang et al., 2016). Climate NA utilized PRISM spatial climate data and used regional climate models (RCM's) to downscale the coarse spatial area for specific locations and elevations (Wang et al., 2016). The RCMs take outputs of larger-scale global climate models (GCMs) and use localized data such as topography, natural phenomena, and surface characteristics to create finer scale

models that are more accurate to a specific region, and which would be lost in the coarser GCM (American Meteorological Society, 2013). The data swapping within FIA to protect plot integrity does not significantly affect climatological data. The mesoscale phenomena would remain relatively constant with only minor changes in the microclimate of the given area. Since all values are 30-year normals, the averaging of data would overcome the effect of small-scale variation. Climate values by FIA plot are shown in Appendix A as maps across the study area.

Specific gravity data were taken from Miles and Smith (2009) who compiled values for species recorded within FIA. For more information on how they obtained that data, please refer to Miles and Smith (2009).

Shade and drought tolerance data were obtained from published sources provided by Niinemets and Valladares (2006). These numerical values ranged from 1-5 and were calculated as averages across life stages and regions for a given species. If a given species did not have tolerance values reported, they were substituted for a similar species native to the study area. Where species was not provided (ex. *Cayra spp.*), an average of the native species listed that occurred within the southeastern US was substituted. In addition, shrub species, species that FIA has dropped from their collection list, and species with no other genus equivalents were also substituted. I chose not to drop invasive tree species if I had reported tolerance values, as removing these might alter the results of the stand dynamics in the region. All SG and functional trait data used in this analysis are reported in Table B1 of Appendix B.

Building an Index using Relative Stand Density

My stand density index based on relative density (SDI_{RD}), was built from the adaptation of Chisman and Schumacher (1940)'s tree area ratio (TAR) equation (equation 9) (Ducey and Knapp, 2010).

$$b_0 x_0 + b_1 x_1 + \varepsilon = 1 \quad (9)$$

Where b_0 and b_1 are stand-specific coefficients, x_0 and x_1 are the summations of individual tree observations in the dataset, with an approximate error constant that is set equal to 1. This model form allows me to regress stand data in a way that compares actual stocking to potential stocking. Each FIA cluster plot was treated as an independent observation and had two summations calculated to fit the regression equation. In equations 10 and 11 below, x0 and x1 represent the calculations of the two summations in equation 9 using an expansion factor (EF) taken from the FIA tables, to convert individual tree observations to a per hectare basis (sensu Ducey and Knapp, 2010):

$$x_0 = \sum_i EF_i (\frac{DBH_i}{25})^{1.6} \quad (10)$$

$$x_1 = \sum_i EF_i SG_i (\frac{DBH_i}{25})^{1.6} \quad (11)$$

These equations were combined to create the model form below to calculate relative density as developed by Ducey and Knapp (2010; Equation 12):

$$RD = b_0 \sum_i \left(\frac{DBH_i}{25}\right)^{1.6} + b_1 \sum_i SG_i \left(\frac{DBH_i}{25}\right)^{1.6} \quad (12)$$

Where DBH_i is the diameter of i^{th} tree, which is then added to this same summation where it is then multiplied by the species average specific gravity (SG_i) of the given species. The EF as

denoted in equations 10 and 11 are dropped from the simplified form of equation 12, but still occur within the summations. The coefficients b_0 and b_1 are stand specific and can be found when setting RD =1. Relative density relates the current stocking level of the stand, through an additive approach, to the potential maximum stocking level (Ducey and Knapp, 2010). A fully stocked stand matching its potential would result in an RD equal to 1, with lower stocking levels falling between 0 and 1. The estimated coefficients vary based on the distribution of diameters when calculating ASDI (b_0) in the first summand, while b_1 changes due to species composition as denoted through change in SG.

Quantile Regression

Quantile regression (QR) was used to model maximum size density lines. The advantages of QR lie in the preliminary assumptions and its ability to evaluate the distribution of the independent variables. While the traditional parametric form assumption exists for the independent variables and their coefficients, the random error does not need to conform to a parametric distribution (Cade and Noon, 2003). The quantile in question is represented by τ, which moves based on the given percentile of the dependent variable that changes based on the output of the model (Cade and Noon, 2003; Ducey et al., 2017; Ducey and Knapp, 2010; Scharf et al., 1998; Yang et al., 2018). For instance, if the τ selected is 0.50, it represents the 50^{th} percentile of the output data which in QR is also the median and the mean (Cade and Noon, 2003).

QR allows for selection of a set quantity of collected data and resists the effects of outliers (Ducey et al., 2017; Scharf et al., 1998). QR allowed me to not worry about the stocking of the plots used as I assumed stocking based on relative density. If the stand met the maximum potential stocking, it would equal 1 in the regression, whereas stands below potential maximum

stocking would return a value between 0 and 1. In a traditional linear regression, every stand would need to be assessed for stocking before use. However, for large datasets such as mine, this was not feasible and so by using quantile regression, I can skip this step. QR allowed me to find a best-fit line when various explanatory variables were used.

Quantile testing was conducted on all initial models to aid in quantile selection and inspect variable significance at every quantile. Increasing the quantile forces a greater proportion of the data beneath the modelled regression line, thereby increasing the amount of data used in the modelling process. A successful model would increase implied maximum stand density with increasing quantile. I tested quantiles 0.99, 0.978, 0.95, 0.85, 0.75, and 0.50 to find the best fit for my implied maximum stocking. My model assumed that a fully stocked stand would show a relative density of 1 which is equivalent to the A-line from traditional stocking charts (Ducey and Knapp, 2010). However, true maximum stand density in practice would most likely be less than 1 and sampled plot sizes of FIA would exacerbate the inflation of the predicted max SDI (Bravo-Oviedo et al., 2018; Ducey and Knapp, 2010; Nelson and Vissage, 2007). Since SDI is applicable on the stand level, some overestimation would occur when translating that down to an FIA plot which I use to represent a stand but in the spatial sense, is not the same. To account for maximum density inflation of my model, I compared my QR of all FIA plots to the existing loblolly pine stand density index, which is calculated using ordinary least-squares regression (Williams 1996). This implied maximum ASDI (imASDI) is calculated using the coefficients of the chosen quantile and the same SG where all trees are assumed to have a DBH of 25cm (equation 13) (Ducey and Knapp, 2010).

$$N = \frac{1}{b_0 + b_1 SG} \tag{13}$$

Where N is the implied maximum ASDI calculated using estimated coefficients from the QR (b_0 and b_1) and the SG of the desired species for which to calculate the maximum. In a single-species stand, N is calculated using the average accepted species-specific gravity and in a mixed-species stand, this value must be calculated as an average based on the species-specific SG of the stand (Ducey and Knapp, 2010). The only functional trait used in initially assessing this maximum quantile was the specific gravity of the given plot (Bravo-Oviedo et al., 2018; Ducey et al., 2017).

Next, I added species-specific, normalized indices of drought and shade tolerance described above. I then scaled each value from 0-1 to make them comparable with the SG values (sensu Bravo-Oviedo et al. 2018). This was done by taking the tolerance values and dividing them by the maximum value of the dataset. Niinemets and Valladares' (2006) original indices utilized a 1-5 scale where a 1 was considered very intolerant and a 5 was considered very tolerant. These values were averages across species' life stages and range distribution and are averaged decimal values. They do note that, traditionally these rankings of shade tolerance are mainly applied to juvenile stages of the lifecycle, but that the relativity of the rankings can be broadly applied across the life of a tree (Niinemets and Valladares, 2006; Valladares and Niinemets, 2008). I then calculated modulators of stress to accompany the tolerance values (Bravo-Oviedo et al., 2018). These two modulators representing drought (dI) and cold stress (cI), allow for observing the effects of local climate on maximum stand density. The normalized indices, by themselves, are representative of the species present within the plot and allowed me to examine the potential influence of both shade and drought tolerance. Tolerance indices account for how well a species can withstand a particular stressor compared to other species. The

stress modulators allow me to simulate the effect of temperature or drought stress on a given species, based on its tolerance value. However, it was suggested that by creating a modifier from climate data as opposed to using continuous data, it simplifies the need for many climate interactions based on several parameters (Bravo-Oviedo et al., 2018). These modifiers are then multiplied to the tolerance indices to create a stress value for each plot. To account for this, climate data acquired from Climate NA were used to create interactions of cold and drought stress on the tolerance of species in the plots (Bravo-Oviedo et al., 2018). Rossi et al. (2007) suggest active xylem growth is arrested by minimum temperatures that typically dictate the growing season in a given location. Since it has previously been shown that the shade tolerance for a species is regulated by the length of the growing season (Laanisto and Niinemets, 2015), I adopted a cold stress modulator (cI) from Bravo-Oviedo et al. (2018), for which I can multiply the normalized shade tolerance, in equation 14.

$$cI = 1 - \frac{Tmin - minTmin}{maxTmin - minTmin} \quad (14)$$

Using monthly averages taken from Climate NA, *Tmin* is the minimum temperature of the coldest month for a given plot location, *minTmin* is the absolute minimum monthly average temperature within the dataset, and *maxTmin* is the absolute warmest minimum average temperature within the dataset. This created a normalized cold stress modulator wherein values close to 1 indicate a high cold stress, which is correlated with cold sites, and values close to 0 are indicative of warmer sites. Next, I created a drought intensity modulator to multiply drought tolerance for a plot by its given drought stress. This simulates the amount of drought stress on a

given species when multiplied by its given drought tolerance value. This was done using a normalized index of maximum vapor pressure deficit (VPD) (equation 15).

$$dI = \frac{maxVPD_i}{absMaxVPD} \tag{15}$$

Where dI is the drought stress modulator, $maxVPD_i$ is the maximum VPD of the given FIA plot, and absMaxVPD is the absolute maximum VPD in the dataset.

Adding these tolerance indices into equation 9 both individually and combined allowed me to observe their influence on RD through model analysis (equations 16, 17, 18, 19, and 20) where RD is calculated in a similar fashion to the tree area ratio, or the total amount of growing space required by the tree in a stand (Chisman and Schumacher, 1940). In another iteration of the model, I followed Bravo-Oviedo et al. (2018) in creating an inverse modulator of cold stress, 1-cI, from here listed as mcI. This flips the stress modulator so that the model becomes more sensitive towards warmer sites where 0 is colder sites and 1 is warmer sites.

$$RD = b_0 \sum_i \left(\frac{DBH_i}{25}\right)^{1.6} + b_1 \sum_i SG_i \left(\frac{DBH_i}{25}\right)^{1.6} + b_2 \sum_i (cI * nST_i) \left(\frac{DBH_i}{25}\right)^{1.6} \tag{16}$$

$$RD = b_0 \sum_i \left(\frac{DBH_i}{25}\right)^{1.6} + b_1 \sum_i SG_i \left(\frac{DBH_i}{25}\right)^{1.6} + b_3 \sum_i ((1 - cI) * nDT_i) \left(\frac{DBH_i}{25}\right)^{1.6} \tag{17}$$

$$RD = b_0 \sum_i \left(\frac{DBH_i}{25}\right)^{1.6} + b_1 \sum_i SG_i \left(\frac{DBH_i}{25}\right)^{1.6} + b_3 \sum_i (dI * nDT_i) \left(\frac{DBH_i}{25}\right)^{1.6} \tag{18}$$

$$RD = b_0 \sum_i \left(\frac{DBH_i}{25}\right)^{1.6} + b_1 \sum_i SG_i \left(\frac{DBH_i}{25}\right)^{1.6} + b_2 \sum_i (cI * nST_i) \left(\frac{DBH_i}{25}\right)^{1.6} + b_3 \sum_i (dI * nDT_i) \left(\frac{DBH_i}{25}\right)^{1.6} \quad (19)$$

$$RD = b_0 \sum_i \left(\frac{DBH_i}{25}\right)^{1.6} + b_1 \sum_i SG_i \left(\frac{DBH_i}{25}\right)^{1.6} + b_2 \sum_i ((1 - cI) * nST_i) \left(\frac{DBH_i}{25}\right)^{1.6} + b_3 \sum_i (dI * nDT_i) \left(\frac{DBH_i}{25}\right)^{1.6} \quad (20)$$

where DBH_i is the diameter of the i^{th} tree, SG_i is the specific gravity of the given species of the i^{th} tree, cI is a normalized cold stress modifier described below, nST is the species-specific normalized shade tolerance, dI is a normalized drought stress modifier described above, and nDT is the species-specific normalized drought tolerance, and the coefficients b_0, b_1, b_2, and b_3 are stand specific. Using the coefficients of equation 20, the quantile was chosen based on the implied maximum ASDI estimate as calculated through equation 13 by adding the shade and drought tolerance terms and multiplying them by zero to observe the effect of no heat stress and no drought stress.

Interactions of Climate

Additive String Model

In an effort to analyze how climate variables interact with functional traits, I developed two different modelling approaches that evaluate additive effects versus multiplicative effects.

The functional traits used did not include the stress modulators that were utilized on shade and drought tolerance of the stress-tolerance models. This was because the stress modulators were designed to test specific hypotheses, whereas this model was designed to find the best predictors. My additive models started with functional traits and added additional climate variables in an additive fashion using the quantile selected by the stress-tolerance selection process. Climate traits were added to the model and selected for those which lowered the BIC score the most in each iteration. Since Climate NA provides 270 different measured and calculated climate parameters, I tested the effect of different climate variables to evaluate the influence of other common parameters. Though similar to the climate parameters evaluated by Ducey et al. (2017), Climate NA variables offer a higher spatial resolution (800m; Table 2). Climate data from Climate NA included annual maximum temperature, annual minimum temperature, annual mean temperature, and growing season length. The sum of annual precipitation, sum of growing season precipitation, growing season mean precipitation, amount of growing season days above 5°C, and the growing season mean temperature were calculated from Climate NA derived data. Additionally, I utilized maximum vapor pressure deficit from PRISM directly, also at a spatial resolution of 800m (PRISM Climate Group, Oregon State University, https://prism.oregonstate.edu, data created Feb 2023, accessed Feb 2023). The combined model form builds from equation 12 without stress modulators, with all functional and climate variables added as shown below in equation 21.

$$RD = b_0 \sum_i \left(\frac{DBH_i}{25}\right)^{1.6} + b_1 \sum_i (SG_i)\left(\frac{DBH_i}{25}\right)^{1.6} + b_2 \sum_i (nST_i)\left(\frac{DBH_i}{25}\right)^{1.6} + b_3 \sum_i (nDT_i)\left(\frac{DBH_i}{25}\right)^{1.6} + CV_1 + \ldots + CV_i \quad (21)$$

Where all symbols were previously defined with the addition of CV_1 as the first climate variable added and continued to the i^{th} climate variable.

Mapping Trends

To observe trends due to temperature across the study area, imASDI was calculated by FIA plot for monocultures of the top five dominant species. Plots that were considered monocultures had 90% or more of the plot's total basal area of a single species. This was done using a modification of equation 13, which is derived from the stress-tolerance model. Equation 22 was used with the coefficients from equation 20, while holding SG, shade, and drought tolerance constant for the species with the observed cold and drought stress modulators calculated by plot (Ducey et al., 2017). Mapping these across the study area allowed me to follow changes due to plot location.

$$N = \frac{1}{b_0 + b_1 SG + b_2(mcI * nST) + b_3(norVPD * nDT)} \quad (22)$$

where SG is the species-specific specific gravity, mcI is the inverse of cold stress, nST is the normalized shade tolerance, norVPD is normalized vapor pressure deficit, nDT is normalized drought tolerance, and b_0, b_1, b_2, and b_3 are calculated coefficients.

Results

The final dataset included 103,884 FIA plot observations with 2,013,326 trees across 186 different species. The 15 most abundant species across the four states by basal area make up 71.64% of the total basal area and 76.36% of the total number of trees. As expected for the

region, loblolly pine (*Pinus taeda*) was the most abundant species accounting for 27.20% of the total basal area and 32.93% of the total tree count. This was followed by sweetgum (*Liquidambar styraciflua*) and slash pine (*Pinus elliottii*) representing 6.89% and 5.44% of the total basal area and 7.95% and 7.75% of the total tree count respectively (Table 1). Across the study area, the maximum annual average temperature was 27.1°C, while the average minimum temperature was 7.9°C. The average total annual precipitation was 1444mm, with 1051mm occurring during the growing season and an average growing season length of 245.8 days (Table 2, Figure 1). Of the 103,884 total plot observations, 23,142 of them are considered monocultures where a single species represents more than 90% of the plot basal area. Of those monoculture plots, more than half (12,529 plots) are pure loblolly pine representing 12% of the total plot observations.

Table 1 Top 15 species by percent abundance across Alabama, Georgia, Louisiana, and Mississippi.

Species	Basal Area, % of total	Trees, % of total	Specific Gravity at 12% MC
Pinus taeda	27.20	32.93	0.51
Liquidambar styraciflua	6.89	7.95	0.52
Pinus elliottii	5.44	7.75	0.59
Quercus nigra	5.33	4.05	0.63
Liriodendron tulipifera	3.49	2.62	0.42
Quercus alba	3.40	2.56	0.68
Pinus echinata	3.03	3.16	0.51
Quercus falcata	2.70	1.96	0.59
Nyssa biflora	2.69	2.95	0.50
Acer rubrum	2.40	3.04	0.54
Pinus palustris	2.30	2.15	0.59
Quercus laurifolia	2.16	1.43	0.63
Nyssa aquatica	1.60	1.02	0.50
Nyssa sylvatica	1.54	1.65	0.50
Quercus prinus	1.46	1.14	0.66

Table 2 Climate variables from Climate NA and PRISM downscaled from 800m for each FIA plot location across Alabama, Georgia, Louisiana, and Mississippi.

Variable	Description	Units	Minimum	Mean	Maximum
AnnMaxTemp	Annual maximum temperature, averaged over years 1991-2020	°C	20.40	27.11	28.70
AnnMinTemp	Annual minimum temperature, averaged over years 1991-2020	°C	0.70	7.97	12.50
AnnPPTSum	Total annual precipitation, averaged over years 1991-2020	mm	1200	1444	2391
AnnTempMean	Mean annual temperature, averaged over years 1991-2020	°C	11.30	17.95	21.10
GSLength	Length of growing season (Frost-free period), averaged over years 1991-2020	days	163	245.8	318
GSPPTSum	Total growing season precipitation, averaged over years 1991-2020	mm	852	1051	1654
GSPPTMean	Mean monthly precipitation during the growing season, averaged over years 1991-2020	mm	94.67	116.80	183.56
GSTempSum	Total growing season degree days above 5C during the growing season, averaged over years 1991-2020	days °C	2632	4381	5130
GSTempMean	Mean monthly temperature during the growing season, averaged over years 1991-2020	°C	14.27	20.91	23.69
maxVPD	Annual maximum vapor pressure deficit, averaged over years 1991-2020	hPa	8.59	16.99	20.31

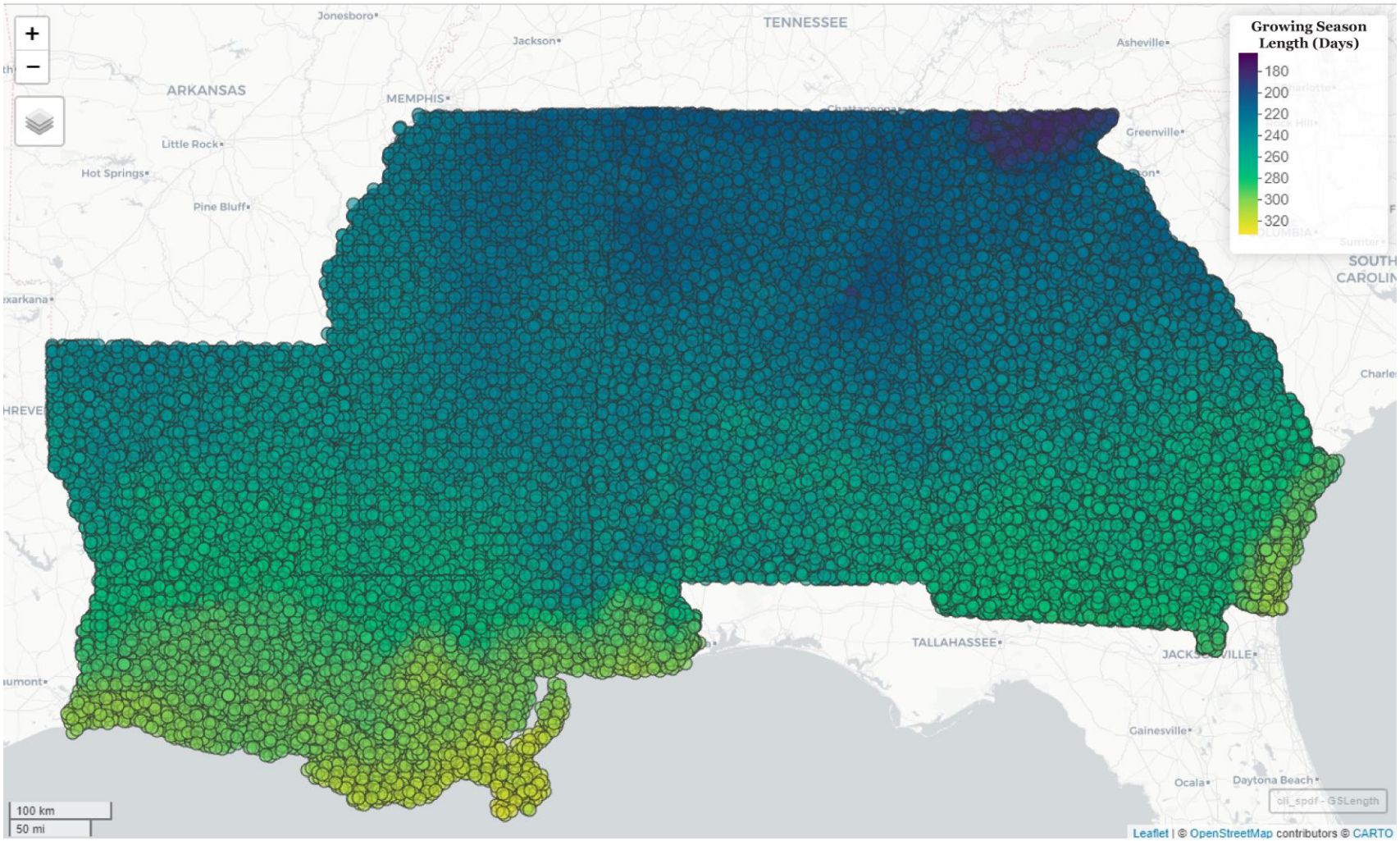

Figure 1 Growing season length (as denoted by the frost-free period) by FIA plot across Alabama, Georgia, Louisiana, and Mississippi.

Both ASDI and SG were found to be significant at all quantiles (Eq. 12). Moving forward to equation 17, shade tolerance and its interaction with cold stress were tested and significant at all quantiles as well. Next, drought tolerance with drought stress was tested using equation 18 and found to be significant at all quantiles. I then tested the combination of both stress tolerance interactions in equation 20. Since the average temperature range of the study area is above freezing (Table 2), I transformed equation 19 into equation 20 by using the inverse of cold stress with shade tolerance. This created a combined model that had functional traits significant at all quantiles with an acceptable range of imASDI for loblolly pine. Significance occurred at every quantile for each variable (Table 3). All model parameters showed significance in the final stress-tolerance model across all quantiles (Eq. 20). The coefficients of the model equation are presented in Table 3.

Table 3 Estimates of coefficients for the stress-tolerance models at every quantile.

Coefficient	Functional Trait	Climate Interaction	50th Quantile (SE)	75th Quantile (SE)	85th Quantile (SE)	95th Quantile (SE)	97.8th Quantile (SE)	99th Quantile (SE)
Base								
b0	-	-	-0.00062 (0.00005)	-0.00079 (0.00004)	-0.00089 (0.00003)	-0.00096 (0.00004)	-0.00107 (0.00005)	-0.00108 (0.00007)
b1	SG	-	0.00562 (0.00010)	0.00494 (0.00007)	0.00473 (0.00006)	0.00432 (0.00007)	0.00423 (0.00009)	0.00405 (0.00012)
Shade Tolerance								
b0	-	-	-0.00055 (0.00005)	-0.00065 (0.00004)	-0.00070 (0.00004)	-0.00070 (0.00003)	-0.00068 (0.00004)	-0.00059 (0.00006)
b1	SG	-	0.00576 (0.00010)	0.00496 (0.00007)	0.00469 (0.00007)	0.00421 (0.00006)	0.00394 (0.00008)	0.00360 (0.00011)
b2	ST	MCI	-0.00051 (0.00005)	-0.00053 (0.00003)	-0.00058 (0.00003)	-0.00069 (0.00003)	-0.00073 (0.00004)	-0.00081 (0.00005)
Drought Tolerance								
b0	-	-	-0.00134 (0.00005)	-0.00133 (0.00004)	-0.00132 (0.00004)	-0.00132 (0.00004)	-0.00131 (0.00004)	-0.00115 (0.00006)
b1	SG	-	0.00579 (0.00009)	0.00509 (0.00007)	0.00480 (0.00006)	0.00436 (0.00006)	0.00411 (0.00008)	0.00359 (0.00010)
b3	DT	Max VPD	0.00109 (0.00003)	0.00080 (0.00002)	0.00069 (0.00002)	0.00061 (0.00002)	0.00060 (0.00002)	0.00063 (0.00003)
Combined								
b0	-	-	-0.00130 (0.00005)	-0.00119 (0.00004)	-0.00118 (0.00004)	-0.00111 (0.00003)	-0.00104 (0.00005)	-0.00093 (0.00004)
b1	SG	-	0.00581 (0.00009)	0.00507 (0.00007)	0.00479 (0.00006)	0.00430 (0.00006)	0.00404 (0.00008)	0.00376 (0.00010)
b2	ST	MCI	-0.00013 (0.00004)	-0.00031 (0.00003)	-0.00034 (0.00003)	-0.00048 (0.00003)	-0.00053 (0.00004)	-0.00060 (0.00005)
b3	DT	Max VPD	0.00107 (0.00003)	0.00073 (0.00002)	0.00063 (0.00002)	0.00054 (0.00002)	0.00046 (0.00003)	0.00047 (0.00003)

Where SG is specific gravity, ST is shade tolerance, MCI is the inverse of cold stress, DT is drought tolerance, and Max VPD is maximum vapor pressure deficit.

For testing implied additive stand density index (imASDI; equation 13), I compared my calculated values to those presented by Williams (1996) for pure stands of loblolly pine with a quadratic mean diameter of 25cm (988 trees/ha). Given the relationship of stand density on small sample plots as noted in Ducey and Knapp (2010), my imASDI is greater than that of the

Williams (1996) guidance, however it presents itself to be sufficiently close (tau = 0.978, imASDI = 983 trees/ha) while retaining a quantile relative of 1 (Fig. 2).

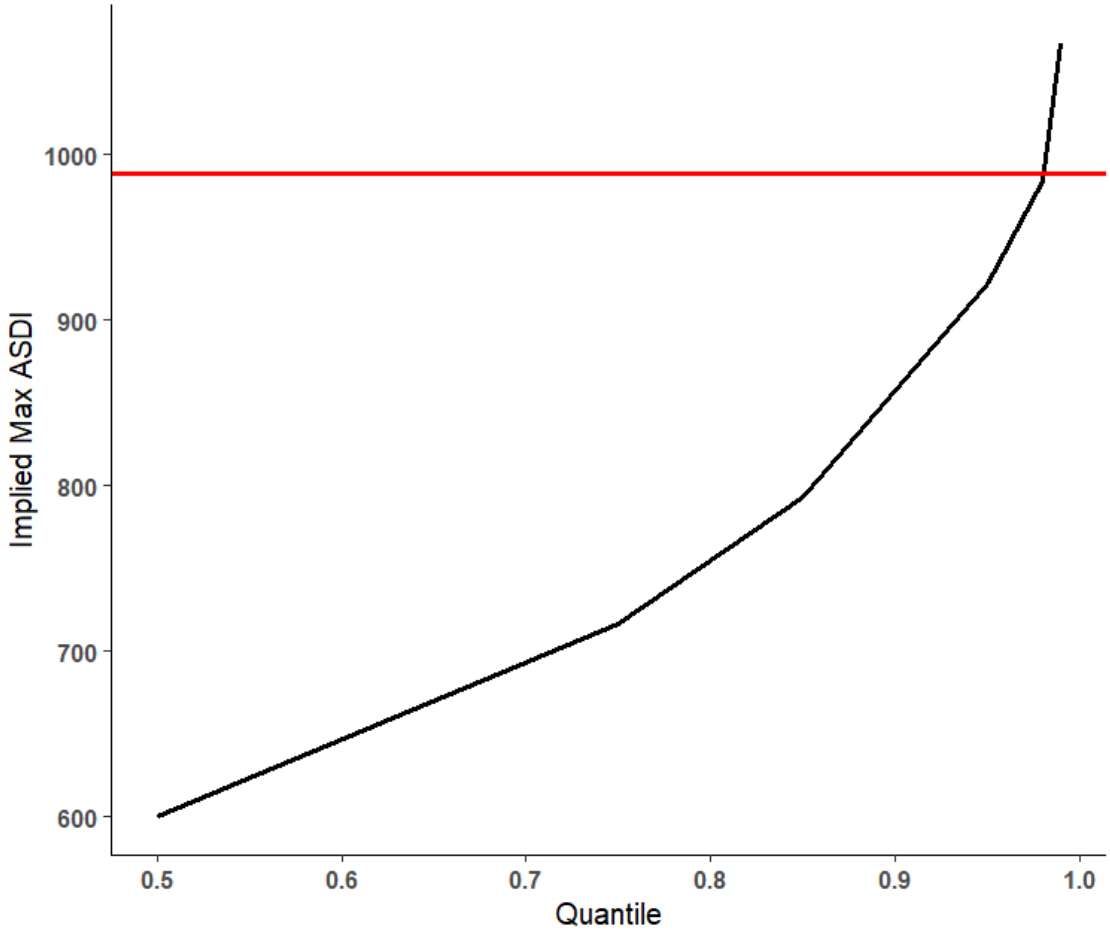

Figure 2 Maximum ASDI calculated at each quantile for loblolly pine. Red line indicates Williams (1996) maximum SDI of 988 trees/hectare.

The best additive model included all functional traits and included all ten climate variables (Table 4). Significant climate variables were: AnnMaxTemp, AnnMinTemp, AnnTempMean, GSLength, GSTempSum, GSTempMean, and maxVPD (Table 4). In the

forward selection process, when only one climate variable was added, annual maximum temperature was the driving variable in BIC. As the stepwise process continued, GSTempSum continued to drive the BIC downwards. The final form showed specific gravity, drought tolerance, AnnPPTSum, GSPPTSum, and GSPPTMean becoming insignificant ($p > 0.05$).

Table 4 Estimates of coefficients for the best additive model with all climate variables added. A * denotes significance ($p<0.05$).

Parameter	Functional Trait	Estimate	Standard Error	P-Value
b0	-	0.00000	0.00000	0.05020
b1	Specific Gravity	0.00000	0.00000	0.74100
b2	Shade Tolerance	0.00000	0.00000	0.00000*
b3	Drought Tolerance	0.00000	0.00000	0.34272
Maximum Annual Temperature	-	0.00336	0.00015	0.00000*
Minimum Annual Temperature	-	-0.00450	0.00012	0.00000*
Total Annual Precipitation	-	0.00000	0.00000	0.66217
Mean Annual Temperature	-	0.01526	0.00048	0.00000*
Growing Season Length	-	0.00008	0.00000	0.00000*
Total Growing Season Precipitation	-	0.00000	0.00002	0.99416
Mean Monthly Precipitation During the Growing Season	-	0.00006	0.00014	0.68957
Growing Season Degree Days Above 5°C	-	-0.00075	0.00000	0.00000*
Mean Monthly Temperature During the Growing Season	-	0.18834	0.00058	0.00000*
Maximum Vapor Pressure Deficit	-	0.00035	0.00002	0.00000*

Mapping the imASDI of each monoculture species showed the spatial distribution of maximum size-density across the four states (Eq.22). Species with higher SG (water oak, *Quercus nigra*) had the lowest range of imASDI with the lowest SG (yellow-poplar, *Liriodendron tulipifera*) had the highest range of imASDI. In order of abundance of basal area, loblolly pine ranged from 762-914 stems/ha, sweetgum ranged from 811-875 stems/ha, slash pine ranged from 664-787 stems/ha, water oak ranged from 609-666 stems/ha, and yellow-poplar ranged from 1266-1458 stems/ha (Fig. 3).

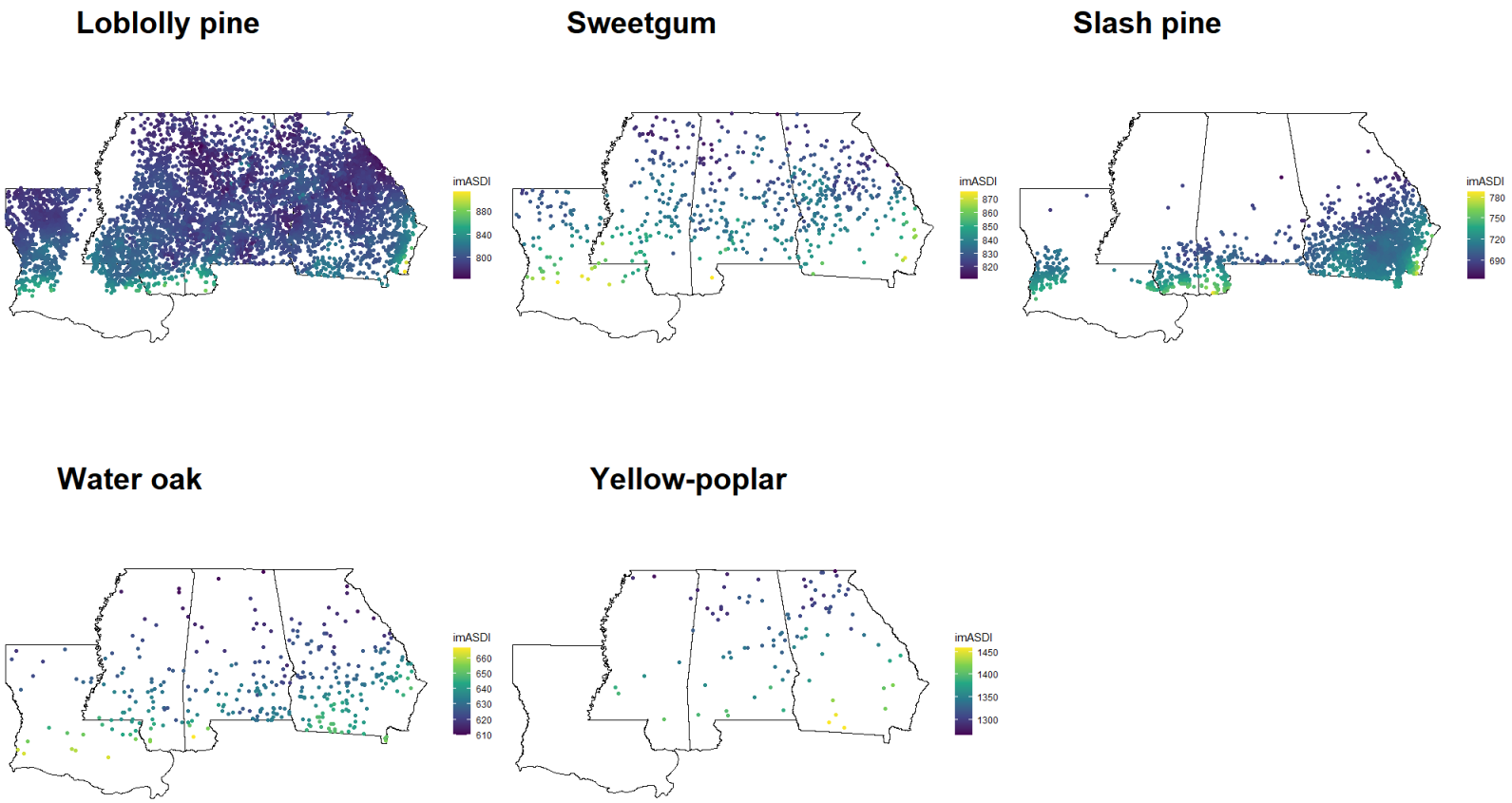

Figure 3 Calculated imASDI (stems/ha) for every monoculture plot of the top five species by basal area across Alabama, Georgia, Louisiana, and Mississippi.

Discussion

My study found that all functional traits (specific gravity, shade tolerance, drought tolerance) were influential in MSDR across the southeastern US. Functional traits also interacted with heat stress and maximum vapor pressure deficit to predict MSDR. I also found that when climate was added to the functional traits, the functional traits lost influence in the model. Temperature was the primary predictor of MSDR, while precipitation was not important across the Southeast.

When SG was added to ASDI in the model with no other functional traits, my results show SG is significant at all quantiles in explaining variation of maximum stand density (Bravo-Oviedo et al, 2018). Species-specific wood SG is related to crown projection area as well as crown structure. This relationship is thought to be a function of mechanical stability. Increased wood SG may also allow species to support longer branches under equal stem and branch sizes, thus allowing for a greater amount of leaf packing per tree (Dean and Baldwin, 1996; Pretzsch, 2019). Further, my predicted RD from the stress-tolerance model of 1050 trees/ha using all species in the study area, is similar to Dean and Baldwin (1996)'s RD of 1110 trees/ha using green SG in pure loblolly stands. While SG became insignificant in the final additive model, it was significant in the stress-tolerance model. The role of specific gravity in the variation of stand density is important especially when considering simple and complex mixtures (Pretzsch et al., 2017). Tree allometry and crown shape dictate the amount of growing space a given tree can occupy, which relate the SG of different species and their crown projection areas (Pretzsch, 2019; Pretzsch et al., 2017). The ability of species to complementarily use available above-and-below ground growing space that monocultures could not utilize was shown to create overyielding in stand volumes through an increase in stand density relative to monocultures

(Pretzsch et al., 2017). I found that, in the additive model, SG became insignificant when climate variables were added. This suggests that the level of influence on MSDR could possibly be better attributed to climate in my study area than the difference of species' SG. One explanation of this is that 27% of the basal area is solely loblolly pine (SG: 0.51). In addition, sweetgum is only 0.01 g/cm^3 different than loblolly (SG: 0.52), meaning that 34% of the total basal area has little variation in SG. The lack of variation, in effect, creates a weighted average based on the species mean SG. This relationship involving SG in the study area is overshadowed by the climate influence.

Examining different species with diverging SG demonstrates the influence of SG in MSDR as shown by the maps in Figure 3. The range of imASDI follows the inverse trend related to species specific SG. Yellow-poplar has the lowest SG at 0.42 g/cm^3 while it has the highest range of imASDI (1266-1458 stems/ha). This trend continues with water oak which has the highest SG of 0.63 and the lowest range of imASDI (609-666 stems/ha). It has previously been shown that SG is sensitive to moisture availability, but that it is also highly heritable (Gilmore et al., 1966; Talbert and Jett, 1981). It is possible that a greater amount of influence due to SG could be seen in loblolly pine if the "regional averages" reported by Talbert and Jett (1981) were used instead of a single average value. While genetic differences may influence SG, the influence of moisture on a given site may change the magnitude of the genetic heritability (Gilmore et al., 1966). These changes in imASDI based on species are supported by Dean and Baldwin (1996)'s hypothesis that SG is a factor in the amount of leaf area that a tree can hold, which would influence the number of stems that can fit on a given hectare (Dean and Baldwin, 1996).

My results also suggest that shade and drought tolerance were important across the Southeast. As higher shade tolerance is related to shorter growing seasons, shade tolerance showed a negative relationship to maximum stand density as my model is sensitive to warmer sites (Laanisto and Niinemets, 2015). This is shown in the significance of inverse cold stress and drought stress when paired with the maximum VPD modifier in the stress-tolerance model. Warmer sites tend to have longer growing seasons and cold sites tend to have shorter growing seasons (Laanisto and Niinemets, 2015). This could potentially be related to latitude shifts as well. With longer growing seasons, drought tolerance becomes more important especially across the east to west gradient as annual precipitation decreases. This shows that species may shift from higher shade tolerance to higher drought tolerance as average temperatures increase (Laanisto and Niinemets, 2015).

Based on these results and those of previous studies, I can assume that in the warmer climate of the southeastern US, shade tolerance is less important than drought tolerance in regulating maximum stand density. A distribution of this trend can be seen in Figure 1 which displays the distribution of growing season length across the study area. Loblolly and slash pine are very tolerant and tolerant to drought respectively, whereas sweetgum is drought intolerant. This can be seen across the landscape as the pines tend to dominate sandy soils which make up the Coastal Plain with loblolly pine reaching into areas of higher clay content mostly due to the industrial nature of its management. However, loblolly pine may also be planted on sites that are not optimal for maximizing stand density. The areas of lower total growing season precipitation overlap well with the areas of highest maximum vapor pressure deficit. Even though shade tolerance was negatively correlated with warmer sites, drought tolerance had a larger influence on MSDR. While drought tolerance was significant across the study area, this may seem

contradictory given the Lower Mississippi Alluvial Valley (LMAV) and the Louisiana swamplands tend to hold water or be inundated for most of the year. Since loblolly pine is absent in most of the LMAV, with generally a larger hardwood presence, I believe that drought tolerance is not nearly as important in the LMAV.

The additive models showed that when climate is added, SG and drought tolerance become insignificant in predicting maximum stand density. Only temperature-related climate variables were significant in the additive model with all functional traits. When built with only one climate variable, AnnMaxTemp had the greatest effect on model performance, followed by GSTempMean for all subsequent steps of the models. This fits with the assumption that productivity in the southeastern US is driven mainly by growing season temperature and not drought as approximately 73% of average annual precipitation (1051 mm of 1444 mm) occurs during the growing season according to Climate NA.

Stockability

It is likely that the proportion of monospecific stands in the dataset has altered the patterns of maximum size density, considering that 22% of the plots within my study area are monospecific. With more than a quarter of the total basal area being loblolly pine, changes in maximum stand density could be related to DeBell et al. (1989)'s concept of stockability. This concept related the differences in stand densities to changes of climate when sites remain relatively similar in site index. My models showed that stand densities are sensitive to environmental factors that may change the onset of self-thinning within a species where it has often been assumed as constant (DeBell et al., 1989). This effect of stockability changed the timing and position of the zone of imminent mortality. Maximum stand density has been shown to increase in both intensively and non-intensively managed plantations with increases in

productivity (Burkhart and Yang, 2022). This has been attributed to a number of factors including improved genetics, site preparation techniques, intermediate treatments, and increased ambient CO_2 (Burkhart and Yang, 2022). However, these do not explain all the variation in RD. Having 270 different species across my study area, I would expect that mixtures would have higher RD than monocultures. This would show functional traits between species having a greater importance than the climate variables, which was not realized. The lack of functional trait importance suggests that stockability of monocultures is more influential to maximum stand density in the southeastern US.

For each species in Figure 3, a latitudinal gradient is observed in the imASDI where stocking increases as the plots get closer to the Gulf of Mexico, indicating variation in stockability. For example, the calculated imASDI for loblolly pine is in line with that of Debell et al., (1989) (762-914 stems/ha vs 850 stems/ha in South Carolina). Should the maximum stocking potential be solely due to silvicultural actions and genetic improvement, it would be logical for loblolly pine to be consistent across the study area as maximum stocking would be independent of site index. However, as this gradient does appear in all five species, this leads me to believe that DeBell's concept of stockability does have merit.

Vapor Pressure Deficit

With climate change changing the average temperature range, the magnitude of diurnal cooling is reduced as summer lows do not reduce to historical levels and increases in minimum temperatures are expected to outpace the increase in maximums (Meehl et al., 2007). On a global scale, precipitation is expected to increase but projections for the southeastern US are less clear (Lee et al., 2021; Meehl et al., 2007). Physiologically, leaves exhibit a boundary layer which can protect them somewhat from this increase in VPD. The boundary layer is an area immediately

around the outside of the leaf where transpiration creates a moisture buffer from the atmospheric conditions surrounding the tree. A boundary layer fueled by canopy transpiration would dampen the effect of atmospheric VPD possibly leading to the observed results. As air VPD increases, the leaf boundary VPD acts as a buffer, and the effects of radiation on leaf temperature becomes much more important in regulating transpiration (Grossiord et al., 2020; Day, 2000; Jarvis and McNaughton, 1986; Marchin et al., 2016). Increased periods of transpiration that are due to elevated VPD could exacerbate drought stress and loss of soil moisture (Duan et al., 2014; Grossiord et al., 2020; Will et al., 2013). This could result in stunted growth from stomatal closure and in the worst cases, could result in hydraulic failure (Cochard, 2021; Grossiord et al., 2020; Will et al., 2013). Thus, the increased atmospheric drought stress and reduced soil moisture predicted into the future would begin to select for species with higher drought tolerance and lower maximum stand densities.

My results show that the southeastern US is believed to be influenced more by temperature than precipitation. However, temperature can affect the availability of water to plants depending on the timing and intensity of precipitation. When added in the additive models, VPD was significant in the final iteration, but was never a large driver of variation. This could potentially be due to the variable being a long-term average, the boundary layer as mentioned by Grossiord et al. (2020), the lack of moisture limitation in the area, or a combination of the three. Given that drought tolerance with the VPD stress modifier showed importance in changing stand densities, I expect to see this become exacerbated in the future, granted the magnitude of this is unknown (Lee et al. (2021) and Meehl et al. (2007)).

VPD in my model, by itself, does not allow me to test for changes in soil moisture content, while other studies have found that stand density was negatively correlated with soil

moisture content (Wei and Liang, 2021). While Wei and Liang (2021) focused on plantations of Chinese pine (*Pinus tabulaeformis*) and black locust (*Robinia pseudoacacia*), their stem densities are similar to loblolly when fully stocked and they found that reducing stand density increased soil moisture while remaining below the soil water carrying capacity. It is thought that stand density drives soil water content in arid systems and is related to leaf area (Wei and Liang, 2021). My study area does not appear to be a moisture-limited system.

Interactions of Climate on Maximum Stand Density in Additive Models

There is high certainty not only that average temperature extremes will widen, but that long-term average temperature increasing on a monthly and annual basis should have negative impacts on stand density (Andrews et al., 2020; Lee et al., 2021; Meehl et al., 2007). Increased temperature can reach a point which has a negative effect on tree growth and stand density. Higher temperatures and periods of associated drought exhibited a larger impact on high density stands than low density stands, as high density stands have more competition for resources (Andrews et al., 2020). This is inconclusive with my model results as monthly mean temperature during the growing season was the most influential climate varaible in the additive model and showed a positive relationship with maximum stand density. Similarly, Anderson-Teixeira et al. (2022) found that mean annual temperature was never an important variable in their climate modelling analysis, however temperature was influential on a shorter temporal scale during the growing season. As they state, one of the more influential variables was daily maximum temperature. This is in line with increasing temperatures having a slowing effect on growth at a certain point (Anderson-Teixeira et al., 2022). Generally, increased temperatures resulted in lower net photosynthesis and increasing dark respiration which would result in carbon loss (Teskey and Will, 1999). Even with acclimation effects to higher temperatures, photosynthetic

capacity can decrease at higher temperatures and resulted in mortality in extreme conditions (Teskey and Will, 1999). This translates to my model as increasing daily maximum temperatures over a long period of time will increase annual and monthly mean temperature during the growing season, plausibly explaining its role in influencing maximum size-density. However, this could be affected by the change in daily minimum temperatures, although these are generally expected to increase based on current projections (Lee et al., 2021; Meehl et al., 2007). With the insignificance of all precipitation climate factors, I assume that my study area is not limited by moisture, even in areas of excessively drained soils.

CHAPTER IV

CONCLUSIONS

Unpacking the Tent

So, what does all this mean in terms of maximum size-density relationships (MSDR)? While I believe that specific gravity (SG) plays a role in species variation across climate gradients, intra-species variation of SG may also play a role in combination with climate to regulate maximum stand density. Intra-species variation in shade and drought tolerance across the range may also be important and assessing the level of this variation may help improve modelling of maximum stand density. However, given my results, this does not seem apparent across the southeastern US. Any variation that exists due to SG is overpowered by the influence of climate on maximum stand density. Given the importance of maximum temperature across the range, I expect that drought tolerance would be most important on an east to west gradient due to changes in moisture regimes. In addition, shade tolerance should show a gradient from north to south when related to maximum stand density. However, my models cannot detect these gradients across plot averages which may obscure more local variation. While many studies have looked at MSDR in loblolly pine plantations in the southeastern US, to my knowledge, no other study has looked at maximum stand density on the individual-tree level using all species data as I have done here.

While some studies have found that my individual-tree, quantile approach tends towards overestimation, I believe my methods are justified (Salas-Eljatib and Weiskittel, 2018), and this

overestimation is due, in part, to the limited stratification applied by the FIA sampling protocol. Given the size of the FIA plots, being small and easily measurable, it is not unreasonable to expect that maximum densities are higher than in real life due to estimation of a stand-level index using individual tree observations. However, based on my model and predicted maximum stand density for loblolly pine, the model only overpredicted above the 98th quantile. For the chosen quantile, the implied maximum stand density was predicted to be approximately 1000 stems/ha with my guidance stating full stocking at 988 stems/ha (Williams, 1996). While an original goal of this exercise was to look at relationships in mixed-species stands as done by Andrews et al. (2018), the industrialized nature of the study area weighted the analysis to examine mainly loblolly pine and its interaction as a monoculture or simple mixtures. While Bravo-Oviedo et al. (2018) removed what they considered to be plots that were "intensively managed plantations", I chose not to do that as to observe the stand dynamics happening across the landscape and not simply in natural stands. Specific gravity may vary within a species' range depending on growth rate, the length of the growing season and variation between provenances. However, these data were not available to me and made testing this unrealistic given current circumstances. Significant differences between loblolly pine provenances and changes in SG were not present, however it has been demonstrated that there is some latitudinal and east/west variation (Jayawickrama et al., 1997; Tauer and Loo-Dinkins, 1990). This small, but important, variation could play a role in changes of maximum stand density across the range and would be an interesting extension to this analysis.

While I used a different method than Andrews et al. (2018), I share much of the same findings as they did in the Acadia region of the northeastern US and Canada, with shade and drought tolerance being important factors of maximum stand density in addition to climate.

While they found that precipitation was an important factor, I also found that mean temperature overall and during the growing season, were important.

In a study on changes in self-thinning lines, Forrester et al. (2021) found that mixtures did not have higher maximum stand densities than monocultures of the same species which contrasts with other findings. For mixtures to overyield, they must be complementary in their use of available growing space or facilitate each other, thus it is difficult to generally assume that all species mixture would overyield. While it has been shown that climate is influential on self-thinning lines and maximum stand density, other drought indices and finer temporal resolution of climate may be necessary for more small-scale variation (Forrester et al., 2021). Uncertainty in future climate makes the addition of climate in maximum stand density models inadvisable to some, due to the bias it may add to future conditions (Forrester et al., 2021). However, based on my results, previous work, and improved confidence in future climate models from the IPCC, not considering the effects of climate is ill-advised (Anderson-Teixeira et al., 2022; Andrews et al., 2018; Burkhart and Yang, 2022). While I show that climate is an important factor affecting stand density, the relationship between soil and water holding capacity is not explored here and could provide additional details for the effect of precipitation.

Canopy position and stand density may change the leaf packing area (Shinozaki et al., 1964). My study assumes a quadratic mean diameter across my stands based on the original Reineke formula, so I therefore assume a roughly constant leaf area for a given species based on the mechanical hypothesis of proportional basal area and specific gravity to leaf area ratio (Dean and Baldwin, 1996; Shinozaki et al., 1964; Woodall et al., 2005). I assume that species, in conjunction with its specific gravity, play a role in leaf area packing across the range, but that climate is more limiting. Based on my results of climatic effects on maximum stand density

being greater than that of specific gravity, I conclude that climate and stockability of a given species on different sites is a driving factor of stand density across the southeastern US. My study has shown that in single-species and simple-mixed stands of the southeastern US, climate has a greater effect on maximum stand density than selected plant functional traits. I also would expect that, in more complex mixtures where niche partitioning allows for a greater development of canopy strata, functional traits may play a larger role in regulating stand density than climate.

Implications for Management

Maximum stand density has broad implications across the landscape for management and stand behavior. With climate change, stand densities will continue to increase in certain areas (Woodall and Weiskittel, 2021) and drought tolerance of species will become increasingly important to stand development across the US. Managers should utilize this information with anticipation of removing more basal area mid-rotation to retain the desired basal area on the landscape, while understanding that drought tolerant species will become more prevalent on an east to west gradient, nationally. In addition, changes to MSDR within a species across a geographic area would influence the timing of thinning treatments. Managers should utilize SDI and MSDR to plan thinning entries based on relative stand position to competition-induced mortality to prevent a loss of productivity (Dean and Baldwin, 1993). My study has shown that stand dynamics across the Southeast appear to be driven by plantation forestry as shown by a lack of effect of functional traits by themselves. Previous studies have shown that mixed stands of complementary species will be able to utilize more available growing space than monocultures alone (Pretzsch et al., 2017). However, our study does not provide a clear answer on this for the southeastern US. Based on current knowledge of climate and functional traits

within trees, it should be anticipated that drought tolerance will become more important to species survival, especially in the western part of the Coastal Plain.

REFERENCES

Alabama Forestry Commission. (n.d.). Retrieved April 21, 2023, from https://www.forestry.alabama.gov/Default.aspx

American Meteorological Society. (2013, July 9). *Regional Cimate Model—Glossary of Meteorology*. https://glossary.ametsoc.org/wiki/Regional_climate_model

Anderson-Teixeira, K. J., Herrmann, V., Rollinson, C. R., Gonzalez, B., Gonzalez-Akre, E. B., Pederson, N., Alexander, M. R., Allen, C. D., Alfaro-Sánchez, R., Awada, T., Baltzer, J. L., Baker, P. J., Birch, J. D., Bunyavejchewin, S., Cherubini, P., Davies, S. J., Dow, C., Helcoski, R., Kašpar, J., … Zuidema, P. A. (2022). Joint effects of climate, tree size, and year on annual tree growth derived from tree-ring records of ten globally distributed forests. *Global Change Biology*, *28*(1), 245–266. https://doi.org/10.1111/gcb.15934

Andrews, C. M., D'Amato, A. W., Fraver, S., Palik, B., Battaglia, M. A., and Bradford, J. B. (2020). Low stand density moderates growth declines during hot droughts in semi-arid forests. *Journal of Applied Ecology*, *57*(6), 1089–1102. https://doi.org/10.1111/1365-2664.13615

Andrews, C., Weiskittel, A., D'Amato, A. W., and Simons-Legaard, E. (2018). Variation in the maximum stand density index and its linkage to climate in mixed species forests of the North American Acadian Region. *Forest Ecology and Management*, *417*, 90–102. https://doi.org/10.1016/j.foreco.2018.02.038

Bechtold, W. A., and Patterson, P. L. (2015). *The Enhanced Forest Inventory and Analysis Program National Sampling Design and Estimation Procedures* (SRS-GTR-80; p. SRS-GTR-80). US Department of Agriculture, Forest Service, Southern Research Station. https://doi.org/10.2737/SRS-GTR-80

Bivand, R., Keitt, T., and Rowlingson, B. (2023). *rgdal: Bindings for the "Geospatial" Data Abstraction Library* (1.6-4). https://CRAN.R-project.org/package=rgdal

Bravo-Oviedo, A., Condés, S., del Río, M., Pretzsch, H., and Ducey, M. J. (2018). Maximum stand density strongly depends on species-specific wood stability, shade and drought tolerance. *Forestry: An International Journal of Forest Research*, *91*(4), 459–469. https://doi.org/10.1093/forestry/cpy006

Burkhart, H. E., and Yang, S.-I. (2022). A retrospective comparison of carrying capacity of two generations of loblolly pine plantations. *Forest Ecology and Management*, *504*, 119834. https://doi.org/10.1016/j.foreco.2021.119834

Cade, B. S., and Noon, B. R. (2003). A gentle introduction to quantile regression for ecologists. *Frontiers in Ecology and the Environment*, *1*(8), 412–420. https://doi.org/10.1890/1540-9295(2003)001[0412:AGITQR]2.0.CO;2

Chisman, H. H., and Schumacher, F. X. (1940). On the tree-area ratio and certain of its applications. *Journal of Forestry*, *38*(4), 311–317. https://doi.org/10.1093/jof/38.4.311

Cochard, H. (2021). A new mechanism for tree mortality due to drought and heatwaves. *Peer Community Journal*, *1*. https://doi.org/10.24072/pcjournal.45

Coulston, J. W., Reams, G. A., McRoberts, R. E., and Smith, W. D. (2006). Practical considerations when using perturbed forest inventory plot locations to develop spatial models: A case study. *In: proceedings of the Sixth Annual Forest Inventory and Analysis Symposium; 2004 September 21-24; Denver, CO. Gen. Tech. Rep. WO-70. Washington, DC: US Department of Agriculture Forest Service. 126p., 070.* https://www.fs.usda.gov/research/treesearch/14248

Curtis, R. O. (1971). A tree area power function and related stand density measures for Douglas-fir. *Forest Science*, *17*(2), 146–159. https://doi.org/10.1093/forestscience/17.2.146

Davis, E. C., Sohngen, B., and Lewis, D. J. (2022). The effect of carbon fertilization on naturally regenerated and planted US forests. *Nature Communications*, *13*(1), Article 1. https://doi.org/10.1038/s41467-022-33196-x

Day, M. E. (2000). Influence of temperature and leaf-to-air vapor pressure deficit on net photosynthesis and stomatal conductance in red spruce (*Picea rubens*). *Tree Physiology*, *20*(1), 57–63. https://doi.org/10.1093/treephys/20.1.57

Dean, T. J., D'Amato, A. W., Palik, B. J., Battaglia, M. A., and Harrington, C. A. (2021). A direct measure of stand density based on stand growth. *Forest Science*, *67*(1), 103–115. https://doi.org/10.1093/forsci/fxaa038

Dean, T. J. (2004). Basal area increment and growth efficiency as functions of canopy dynamics and stem mechanics. *Forest Science*, *50*(1), 106–116. https://doi.org/10.1093/forestscience/50.1.106

Dean, T. J., and Baldwin, V. C. (1996). The relationship between Reineke's stand-density index and physical stem mechanics. *Forest Ecology and Management*, *81*(1), 25–34. https://doi.org/10.1016/0378-1127(95)03666-0

Dean, T. J., and Baldwin, V. C. (1993). Using a density-management diagram to develop thinning schedules for loblolly pine plantations. *Res. Pap. SO-275. New Orleans, LA: US Department of Agriculture, Forest Service, Southern Forest Experiment Station. 12 p., 275*. https://doi.org/10.2737/SO-RP-275

DeBell, D. S., Harms, W. R., and Whitesell, C. D. (1989). Stockability: A major factor in productivity differences between *Pinus taeda* plantations in Hawaii and the southeastern United States. *Forest Science*, *35*(3), 708–719. https://doi.org/10.1093/forestscience/35.3.708

del Río, M., Bravo-Oviedo, A., Ruiz-Peinado, R., and Condés, S. (2019). Tree allometry variation in response to intra- and inter-specific competitions. *Trees*, *33*(1), 121–138. https://doi.org/10.1007/s00468-018-1763-3

Duan, H., Duursma, R. A., Huang, G., Smith, R. A., Choat, B., O'grady, A. P., and Tissue, D. T. (2014). Elevated [CO_2] does not ameliorate the negative effects of elevated temperature on drought-induced mortality in *Eucalyptus radiata* seedlings. *Plant, Cell and Environment*, *37*(7), 1598–1613. https://doi.org/10.1111/pce.12260

Ducey, M. J., and Knapp, R. A. (2010). A stand density index for complex mixed species forests in the northeastern United States. *Forest Ecology and Management*, *260*(9), 1613–1622. https://doi.org/10.1016/j.foreco.2010.08.014

Ducey, M. J., and Larson, B. C. (2003). Is there a correct stand density index? An alternate interpretation. *Western Journal of Applied Forestry*, *18*(3), 179–184. https://doi.org/10.1093/wjaf/18.3.179

Ducey, M. J., Woodall, C. W., and Bravo-Oviedo, A. (2017). Climate and species functional traits influence maximum live tree stocking in the Lake States, USA. *Forest Ecology and Management*, *386*, 51–61. https://doi.org/10.1016/j.foreco.2016.12.007

Forrester, D. I., Baker, T. G., Elms, S. R., Hobi, M. L., Ouyang, S., Wiedemann, J. C., Xiang, W., Zell, J., and Pulkkinen, M. (2021). Self-thinning tree mortality models that account for vertical stand structure, species mixing and climate. *Forest Ecology and Management*, *487*, 118936. https://doi.org/10.1016/j.foreco.2021.118936

Gauli, A., Neupane, P. R., Mundhenk, P., and Köhl, M. (2022). Effect of climate change on the growth of tree species: Dendroclimatological Analysis. *Forests*, *13*(4), Article 4. https://doi.org/10.3390/f13040496

Georgia Forestry Commission. (202 C.E., November 15). https://gatrees.org/

Gilmore, A. R., Boyce, S. G., and Ryker, R. A. (1966). The relationship of specific gravity of loblolly pine to environmental factors in southern Illinois. *Forest Science*, *12*(4), 399–405. https://doi.org/10.1093/forestscience/12.4.399

Grossiord, C., Buckley, T. N., Cernusak, L. A., Novick, K. A., Poulter, B., Siegwolf, R. T. W., Sperry, J. S., and McDowell, N. G. (2020). Plant responses to rising vapor pressure deficit. *New Phytologist*, *226*(6), 1550–1566. https://doi.org/10.1111/nph.16485

Hancock, D., Harris, G., Franks, R., Morgan, S., and Green, T. W. (2014). *Soil and fertilizer management considerations for forage systems in Georgia: Bulletin 1346* (Bulletin No. 1346). University of Georgia Extension. https://extension.uga.edu/publications/detail.html?number=B1346&title=soil-and-fertilizer-management-considerations-for-forage-systems-in-georgia#Types

Hatfield, J. L., and Prueger, J. H. (2015). Temperature extremes: Effect on plant growth and development. *Weather and Climate Extremes*, *10*, 4–10. https://doi.org/10.1016/j.wace.2015.08.001

Hijmans, R. (2023). *raster: Geographic Data Analysis and Modeling* (3.6-14). https://CRAN.R-project.org/package=raster

Iannone, R., Cheng, J., Schloerke, B., Hughes, E., and Seo, J. (2022). *gt: Easily Create Presentation-Ready Display Tables* (0.8.0). https://CRAN.R-project.org/package=gt

Jarvis, P. G., and McNaughton, K. G. (1986). Stomatal control of transpiration: Scaling up from leaf to region. In A. MacFadyen and E. D. Ford (Eds.), *Advances in Ecological Research* (Vol. 15, pp. 1–49). Academic Press. https://doi.org/10.1016/S0065-2504(08)60119-1

Jayawickrama, K. J., McKeand, S. E., Jett, J. B., and Wheeler, E. A. (1997). Date of earlywood-latewood transition in provenances and families of loblolly pine, and its relationship to growth phenology and juvenile wood specific gravity. *Canadian Journal of Forest Research*, *27*(8), 1245–1253. https://doi.org/10.1139/x97-091

Keenan, T. F., Gray, J., Friedl, M. A., Toomey, M., Bohrer, G., Hollinger, D. Y., Munger, J. W., O'Keefe, J., Schmid, H. P., Wing, I. S., Yang, B., and Richardson, A. D. (2014). Net carbon uptake has increased through warming-induced changes in temperate forest phenology. *Nature Climate Change*, *4*(7), Article 7. https://doi.org/10.1038/nclimate2253

Koenker, R. (2022). *quantreg: Quantile Regression* (5.94). https://CRAN.R-project.org/package=quantreg

Kushla, J. D., and Oldham, L. (2020). *MSU Extension Publication P2822: Forest Soils of Mississippi* (Extension Publication No. P2822; pp. 1–8). Mississippi State University Extension. http://extension.msstate.edu/publications/forest-soils-mississippi

Kweon, D., and Comeau, P. G. (2021). Climate, site conditions, and stand characteristics influence maximum size-density relationships in Korean red pine (*Pinus densiflora*) and Mongolian oak (*Quercus mongolica*) stands, South Korea. *Forest Ecology and Management*, *502*, 119727. https://doi.org/10.1016/j.foreco.2021.119727

Laanisto, L., and Niinemets, Ü. (2015). Polytolerance to abiotic stresses: How universal is the shade–drought tolerance trade-off in woody species? *Global Ecology and Biogeography*, *24*(5), 571–580. https://doi.org/10.1111/geb.12288

Lawrence, M. G. (2005). The relationship between relative humidity and the dewpoint temperature in moist air: A simple conversion and applications. *Bulletin of the American Meteorological Society*, *86*(2), 225–234. https://doi.org/10.1175/BAMS-86-2-225

Lee, J.-Y., Marotzke, J., Bala, G., Cao, L., Corti, S., Dunne, J. P., Engelbrecht, F., Fischer, E., Fyfe, J. C., Jones, C., Maycock, A., Mutemi, J., Ndiaye, O., Panickal, S., and Zhou, T. (2021). Future global climate: Scenario-based projections and near-term information. In V. Masson-Delmotte, P. Zhai, A. Pirani, S. L. Connors, C. Péan, S. Berger, N. Caud, Y. Chen, L. Goldfarb, M. I. Gomis, M. Huang, K. Leitzell, E. Lonnoy, J. B. R. Matthews, T. K. Maycock, T. Waterfield, Ö. Yelekçi, R. Yu, and B. Zhou (Eds.), *Climate Change 2021: The physical science basis. Contribution of working group I to the sixth assessment report of the Intergovernmental Panel on Climate Change* (pp. 553–672). Cambridge University Press. https://doi.org/10.1017/9781009157896.001

Lister, A., Scott, C., King, S., Hoppus, M., Butler, B., and Griffith, D. (2005). Strategies for Preserving Owner Privacy in the National Information Management System of the USDA Forest Service's Forest Inventory and Analysis Unit. In: McRoberts, Ronald E.; Reams, Gregory A.; Van Deusen, Paul C.; McWilliams, William H.; Cieszewski, Chris J., Eds. *Proceedings of the Fourth Annual Forest Inventory and Analysis Symposium; Gen. Tech. Rep. NC-252.* St. Paul, MN: US Department of Agriculture, Forest Service, North Central Research Station. 163-166, 252. https://www.fs.usda.gov/research/treesearch/14404

Long, J. N. (1985). A practical approach to density management. *The Forestry Chronicle*, *61*(1), 23–27. https://doi.org/10.5558/tfc61023-1

Long, J. N., and Daniel, T. W. (1990). Assessment of growing stock in uneven-aged stands. *Western Journal of Applied Forestry*, *5*(3), 93–96. https://doi.org/10.1093/wjaf/5.3.93

Louisiana Department of Agriculture and Forestry. (n.d.). *Department of Agriculture and Forestry*. Retrieved April 21, 2023, from https://www.ldaf.state.la.us/forestry/

Marchin, R. M., Broadhead, A. A., Bostic, L. E., Dunn, R. R., and Hoffmann, W. A. (2016). Stomatal acclimation to vapour pressure deficit doubles transpiration of small tree seedlings with warming. *Plant, Cell and Environment*, *39*(10), 2221–2234. https://doi.org/10.1111/pce.12790

McNulty, S., and Gavazzi, M. (2022). *Southeastern Climate* [Factsheet]. Southeast Regional Climate Hub, USDA. https://www.climatehubs.usda.gov/hubs/southeast/about/

Meehl, G. A., Stocker, T. F., Collins, W. D., Friedlingstein, P., Gaye, A. T., Gregory, J. M., Kitoh, A., Knutti, R., Murphy, J. M., Noda, A., Raper, S. C. B., Watterson, I. G., Weaver, A. J., and Zhao, Z.-C. (2007). Global climate projections. In *climate change 2007: The physical science basis. Contribution of working group I to the fourth assessment report of the Intergovernmental Panel on Climate Change* (pp. 747–846). Cambridge University Press.

Miles, P. D., and Smith, W. B. (2009). Specific gravity and other properties of wood and bark for 156 tree species found in North America. *Res. Note NRS-38. Newtown Square, PA: US Department of Agriculture, Forest Service, Northern Research Station. 35 p.*, *38*, 1–35. https://doi.org/10.2737/NRS-RN-38

Mississippi Forestry Commission. (n.d.). Mississippi Forestry Commission. Retrieved April 21, 2023, from https://www.mfc.ms.gov/

Mitchell, Jr., C. (2008). *Soils of Alabama, ANR-0340* (Extension Publication ANR-0340). Alabama Cooperative Extension System. https://www.aces.edu/wp-content/uploads/2018/12/ANR-0340.REV_.2.pdf

Nelson, M. D., and Vissage, J. (2007). Mapping forest inventory and analysis forest land use: Timberland, reserved forest land, and other forest land. In: McRoberts, Ronald E.; Reams, Gregory A.; Van Deusen, Paul C.; McWilliams, William H., Eds. Proceedings of the Seventh Annual Forest Inventory and Analysis Symposium*; October 3-6, 2005; Portland, ME. Gen. Tech. Rep. WO-77. Washington, DC: US Department of Agriculture, Forest Service: 185-191.*, *77*. https://www.fs.usda.gov/research/treesearch/17041

Niinemets, Ü., and Valladares, F. (2006). Tolerance to shade, drought, and waterlogging of temperate northern hemisphere trees and shrubs. *Ecological Monographs*, *76*(4), 521–547. https://doi.org/10.1890/0012-9615(2006)076[0521:TTSDAW]2.0.CO;2

PRISM Climate Group, Oregon State University. (n.d.). Retrieved February 14, 2022, from https://prism.oregonstate.edu/

Pretzsch, H. (2019). The effect of tree crown allometry on community dynamics in mixed-species stands versus monocultures. A review and perspectives for modeling and silvicultural regulation. *Forests*, *10*(9), Article 9. https://doi.org/10.3390/f10090810

Pretzsch, H., Forrester, D. I., and Bauhus, J. (Eds.). (2017). *Mixed-Species Forests*. Springer. https://doi.org/10.1007/978-3-662-54553-9

Reineke, L. H. (1933). Perfection a stand-density index for even-aged forest. *Journal of Agricultural Research*, *46*, 627–638.

R Core Team. (2021). R: A language and environment for statistical computing. R Foundation for Statistical Computing. https://www.R-project.org/

Robinson, D., Hayes, A., and Couch, S. (2023). *broom: Convert Statistical Objects into Tidy Tibbles* (1.0.3). https://CRAN.R-project.org/package=broom

Rossi, S., Deslauriers, A., Anfodillo, T., and Carraro, V. (2007). Evidence of threshold temperatures for xylogenesis in conifers at high altitudes. *Oecologia*, *152*(1), 1–12. https://doi.org/10.1007/s00442-006-0625-7

Salas-Eljatib, C., and Weiskittel, A. R. (2018). Evaluation of modeling strategies for assessing self-thinning behavior and carrying capacity. *Ecology and Evolution*, *8*(22), 10768–10779. https://doi.org/10.1002/ece3.4525

Scharf, F. S., Juanes, F., and Sutherland, M. (1998). Inferring ecological relationships from the edges of scatter diagrams: Comparison of regression techniques. *Ecology*, *79*(2), 448–460. https://doi.org/10.1890/0012-9658(1998)079[0448:IERFTE]2.0.CO;2

Shaw, J. D. (2000). Application of stand density index to irregularly structured stands. *Western Journal of Applied Forestry*, *15*(1), 40–42.

Shinozaki, K., Yoda, K., Hozumi, K., and Kira, T. (1964). A quantitative analysis of plant form-the Pipe Model Theory: Further Evidence of the Theory and Its Application in Forest Ecology. *14*(4), 133–139. https://doi.org/10.18960/seitai.14.4_133

Stanke, H., Finley, A. O., Weed, A. S., Walters, B. F., and Domke, G. M. (2020). RFIA: An R package for estimation of forest attributes with the US Forest Inventory and Analysis database. Environmental Modelling and Software, 127, 104664.

Talbert, J. T., and Jett, J. B. (1981). Regional specific gravity values for plantation grown loblolly pine in the southeastern United States. *Forest Science*, *27*(4), 801–807. https://doi.org/10.1093/forestscience/27.4.801

Tauer, C. G., and Loo-Dinkins, J. A. (1990). Seed source variation in specific gravity of loblolly pine grown in a common environment in Arkansas. *Forest Science*, *36*(4), 1133–1145. https://doi.org/10.1093/forestscience/36.4.1133

Teskey, R. O., and Will, R. E. (1999). Acclimation of loblolly pine (*Pinus taeda*) seedlings to high temperatures. *Tree Physiology*, *19*(8), 519–525. https://doi.org/10.1093/treephys/19.8.519

US Department of Agriculture, Forest Service, Northern Research Station. (2023). *Forest Inventory and Analysis* (2.0) [Data set]. https://apps.fs.usda.gov/fia/datamart/datamart.html

USDA Forest Service. (2022). *USDA Forest Service, 2022. Forest Inventory and Analysis National Core Field Guide for Standard Measurements, Version 9.2.* US Department of Agriculture, Forest Service. https://www.fia.fs.usda.gov/library/field-guides-methods-proc/index.php

Valladares, F., and Niinemets, Ü. (2008). Shade tolerance, a key plant feature of complex nature and consequences. *Annual Review of Ecology, Evolution, and Systematics*, *39*(1), 237–257. https://doi.org/10.1146/annurev.ecolsys.39.110707.173506

Wang, T., Hamann, A., Spittlehouse, D., and Carroll, C. (2016). Locally downscaled and spatially customizable climate data for historical and future periods for North America. *PLOS ONE*, *11*(6), e0156720. https://doi.org/10.1371/journal.pone.0156720

Wei, X., and Liang, W. (2021). Regulation of stand density alters forest structure and soil moisture during afforestation with *Robinia pseudoacacia L.* and *Pinus tabulaeformis Carr.* on the Loess Plateau. *Forest Ecology and Management*, *491*, 119196. https://doi.org/10.1016/j.foreco.2021.119196

Weindorf, D. C. (2008). *An Update of the Field Guide to Louisiana Soil Classification—LSU AgCenter Research Bulletin #889* (Research Bulletin No. 889; pp. 1–40). Louisiana State University AgCenter. https://www.lsuagcenter.com/~/media/system/2/1/6/8/2168fb704060982327c48305c6c39f2d/b889soilclassificationhighres.pdf

Weiskittel, A. R., and Kuehne, C. (2019). Evaluating and modeling variation in site-level maximum carrying capacity of mixed-species forest stands in the Acadian Region of northeastern North America. *The Forestry Chronicle*, *95*(03), 171–182. https://doi.org/10.5558/tfc2019-026

Wickham, H. (2016). ggplot2: Elegant graphics for data analysis. Springer-Verlag New York. https://ggplot2.tidyverse.org

Wickham, H. (2021). *conflicted: An alternative conflict resolution strategy* (1.1.0). https://CRAN.R-project.org/package=conflicted

Wickham, H., Averick, M., and Bryan, J. (2019). Welcome to the Tidyverse (4(43)). Journal of Open Source Software. https://doi.org/10.21105/joss.01686

Will, R. E., Wilson, S. M., Zou, C. B., and Hennessey, T. C. (2013). Increased vapor pressure deficit due to higher temperature leads to greater transpiration and faster mortality during drought for tree seedlings common to the forest–grassland ecotone. *New Phytologist*, *200*(2), 366–374. https://doi.org/10.1111/nph.12321

Williams, R. A. (1996). Stand density index for loblolly pine plantations in north Louisiana. *Southern Journal of Applied Forestry*, *20*(2), 110–113. https://doi.org/10.1093/sjaf/20.2.110

Woodall, C. W., Miles, P. D., and Vissage, J. S. (2005). Determining maximum stand density index in mixed species stands for strategic-scale stocking assessments. *Forest Ecology and Management*, *216*(1), 367–377. https://doi.org/10.1016/j.foreco.2005.05.050

Woodall, C. W., and Weiskittel, A. R. (2021). Relative density of United States forests has shifted to higher levels over last two decades with important implications for future dynamics. *Scientific Reports*, *11*(1), 18848. https://doi.org/10.1038/s41598-021-98244-w

Yang, T.-R., Lam, T. Y., and Kershaw, J. A. (2018). Developing relative stand density index for structurally complex mixed species cypress and pine forests. *Forest Ecology and Management*, *409*, 425–433. https://doi.org/10.1016/j.foreco.2017.11.043

Yoda, K., Kira, T., Ogawa, H., and Hozumi, K. (1963). Self-thinning in overcrowded pure stands under cultivated and natural conditions. *Journal of Biology, Osaka City University*, *14*, 107–129.

APPENDIX A

CLIMATE MAPS

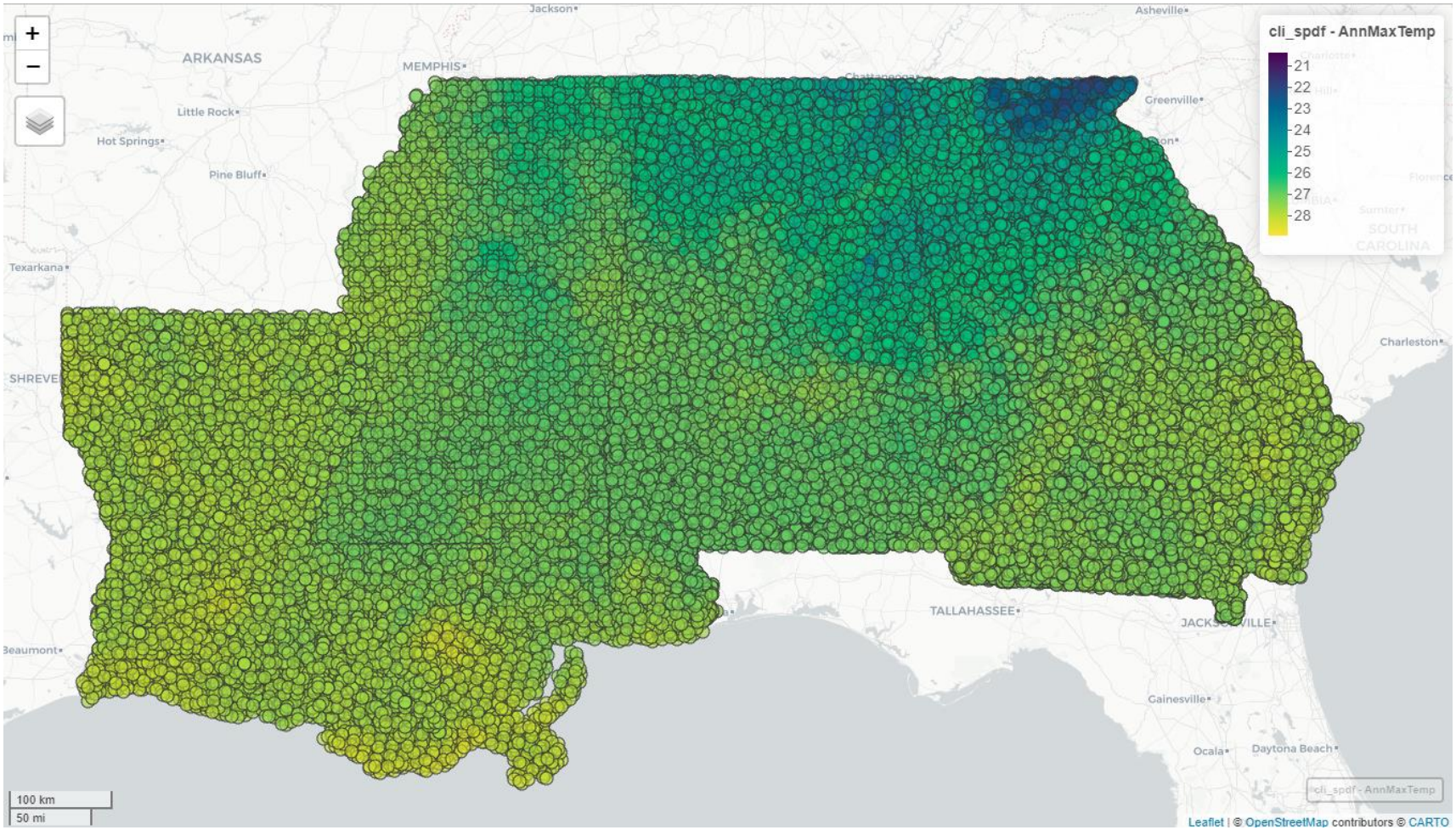

Figure 4 Annual maximum temperature by FIA plot across Alabama, Georgia, Louisiana, and Mississippi.

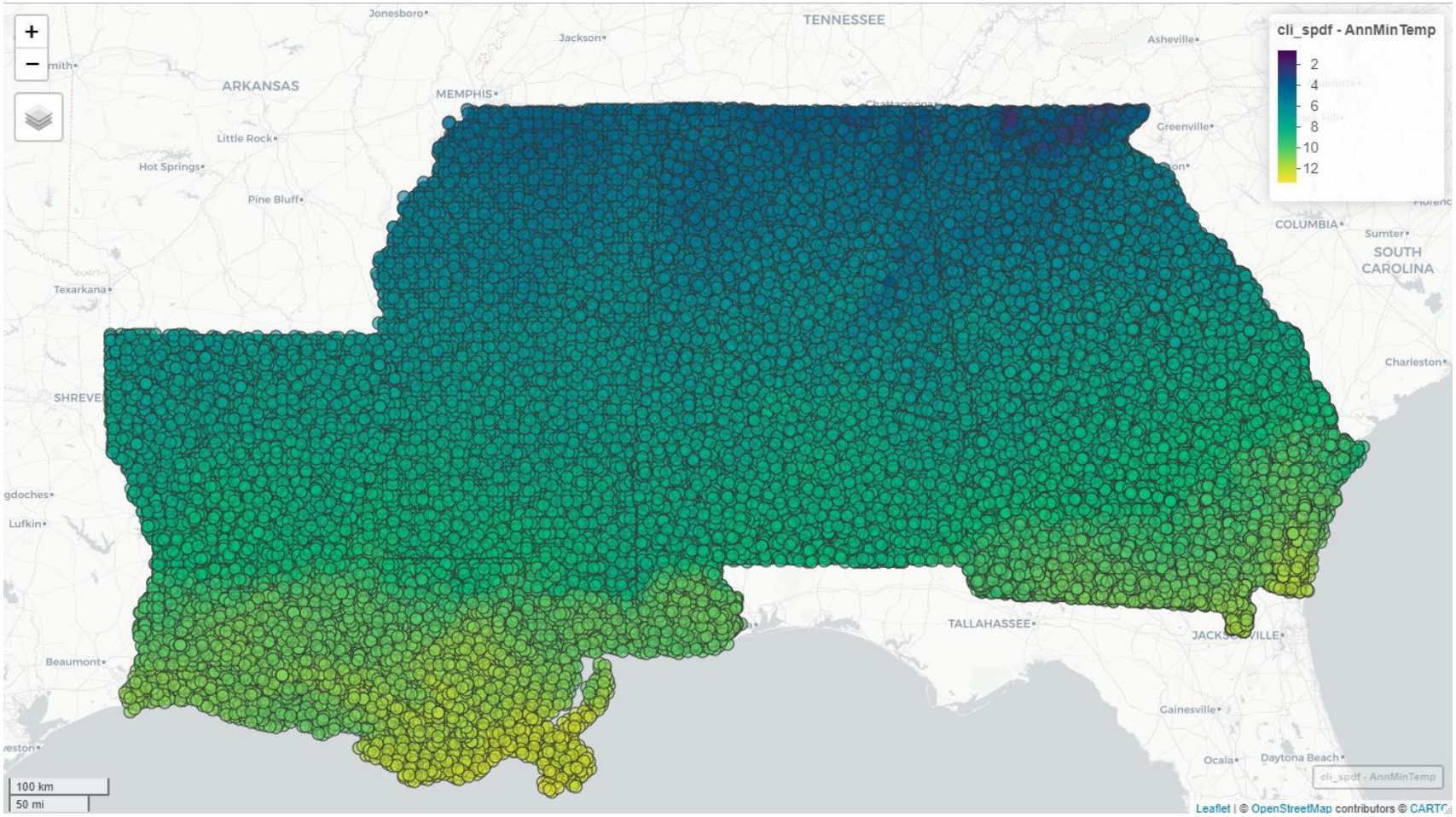

Figure 5 Annual minimum temperature by FIA plot across Alabama, Georgia, Louisiana, and Mississippi.

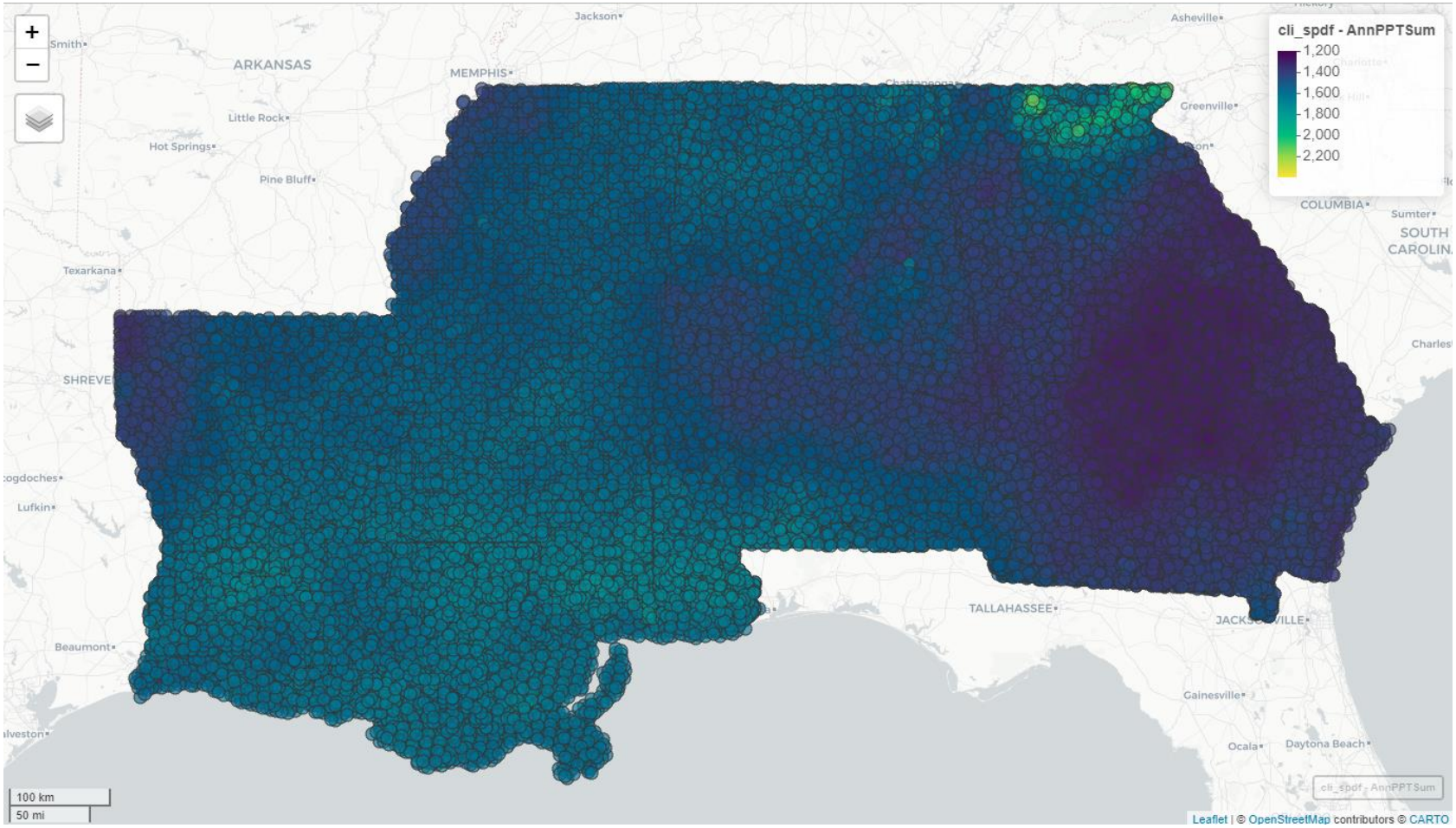

Figure 6 Total annual precipitation by FIA plot across Alabama, Georgia, Louisiana, and Mississippi.

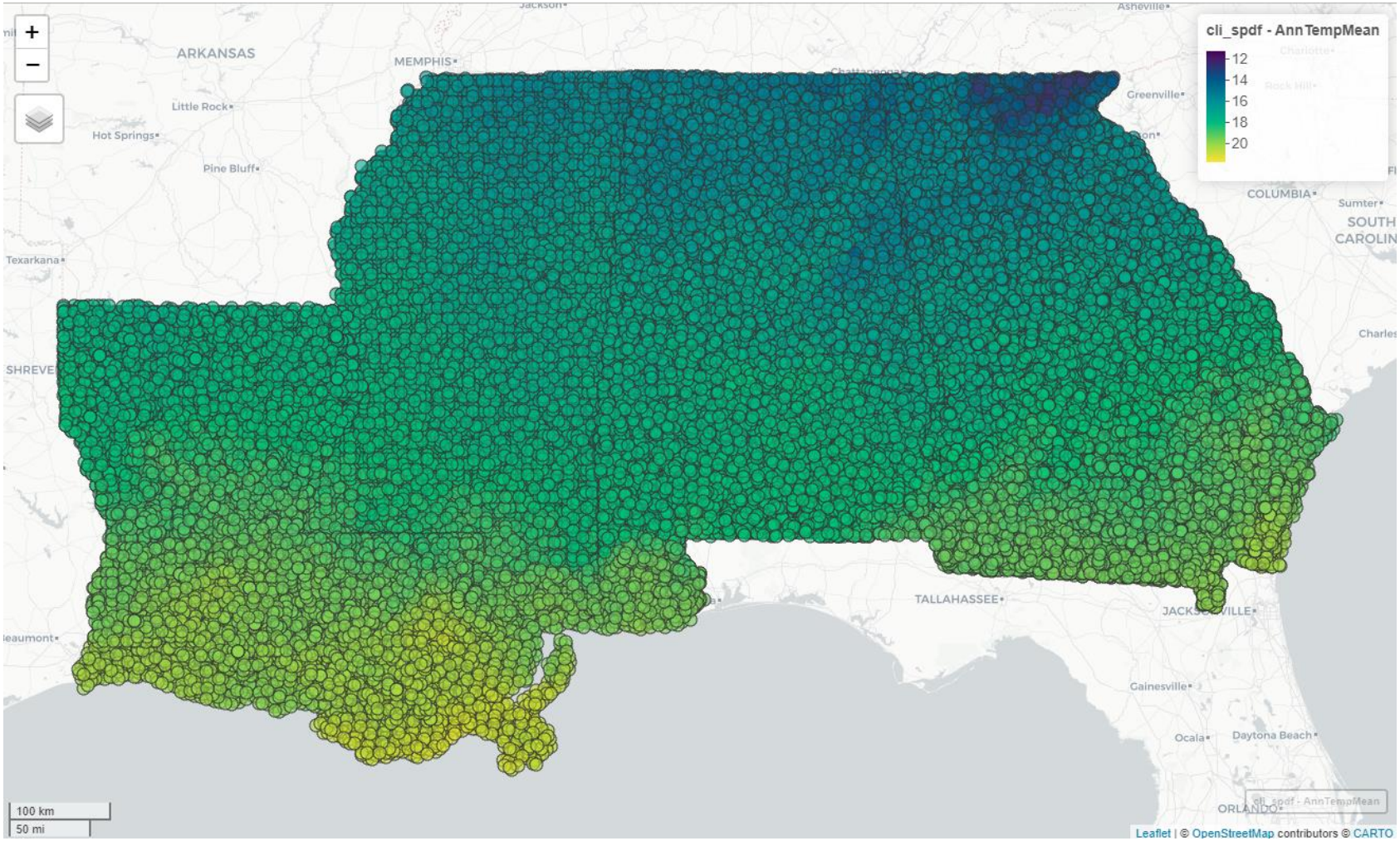

Figure 7 Mean annual temperature by FIA plot across Alabama, Georgia, Louisiana, and Mississippi.

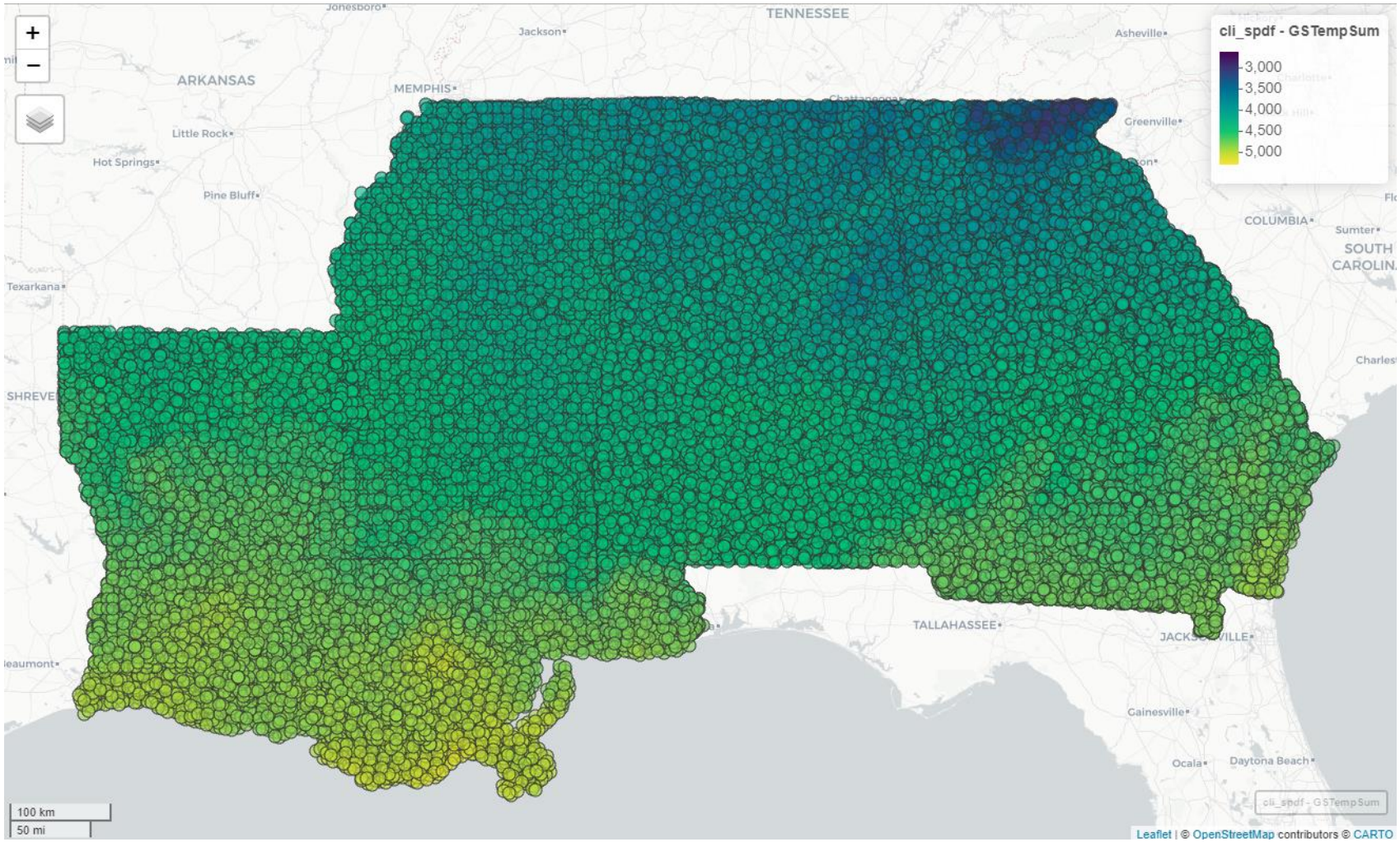

Figure 8 Growing degree days above 5°C excluding meteorological winter by FIA plot across Alabama, Georgia, Louisiana, and Mississippi.

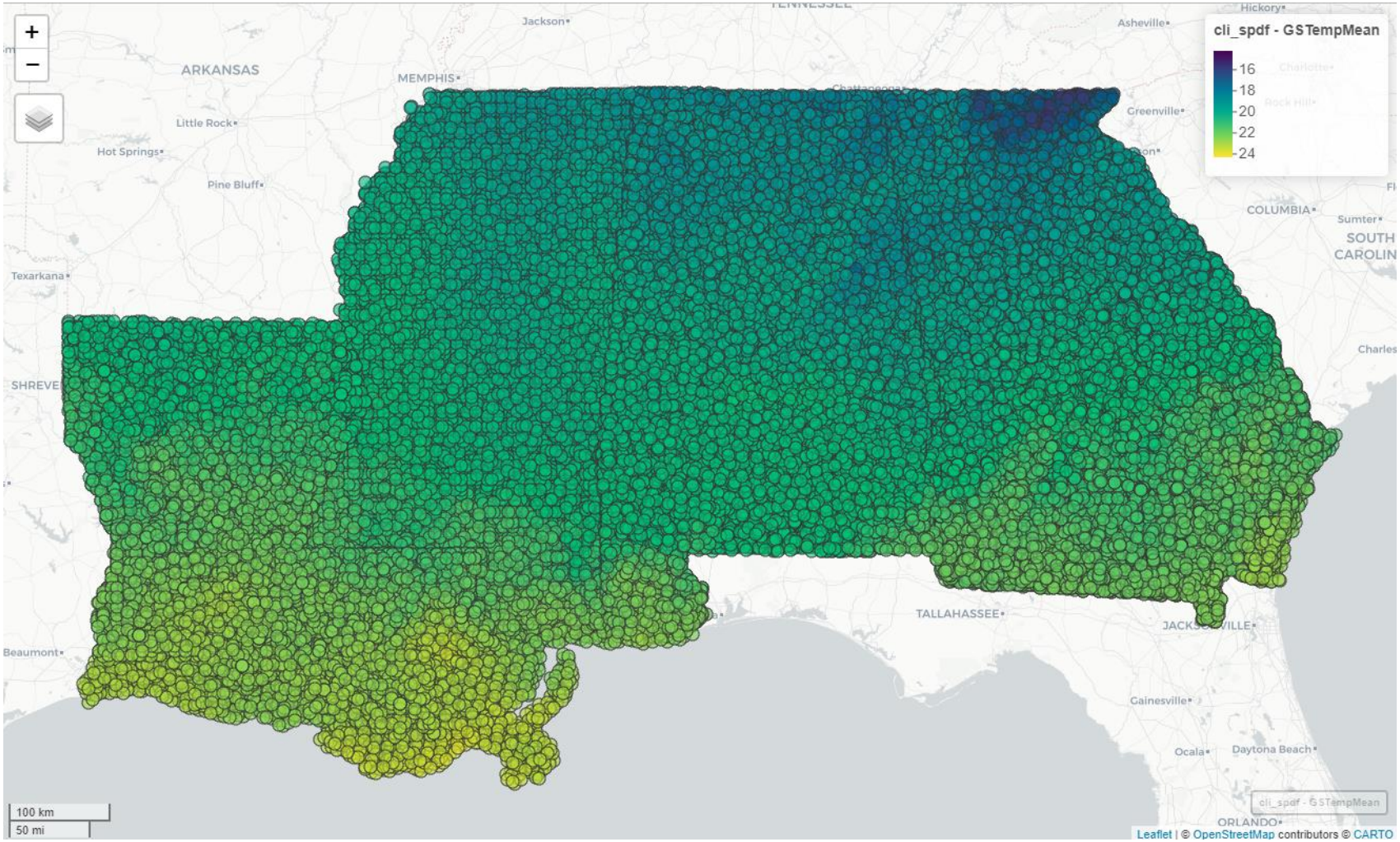

Figure 9 Mean monthly temperature during the growing season by FIA plot across Alabama, Georgia, Louisiana, and Mississippi.

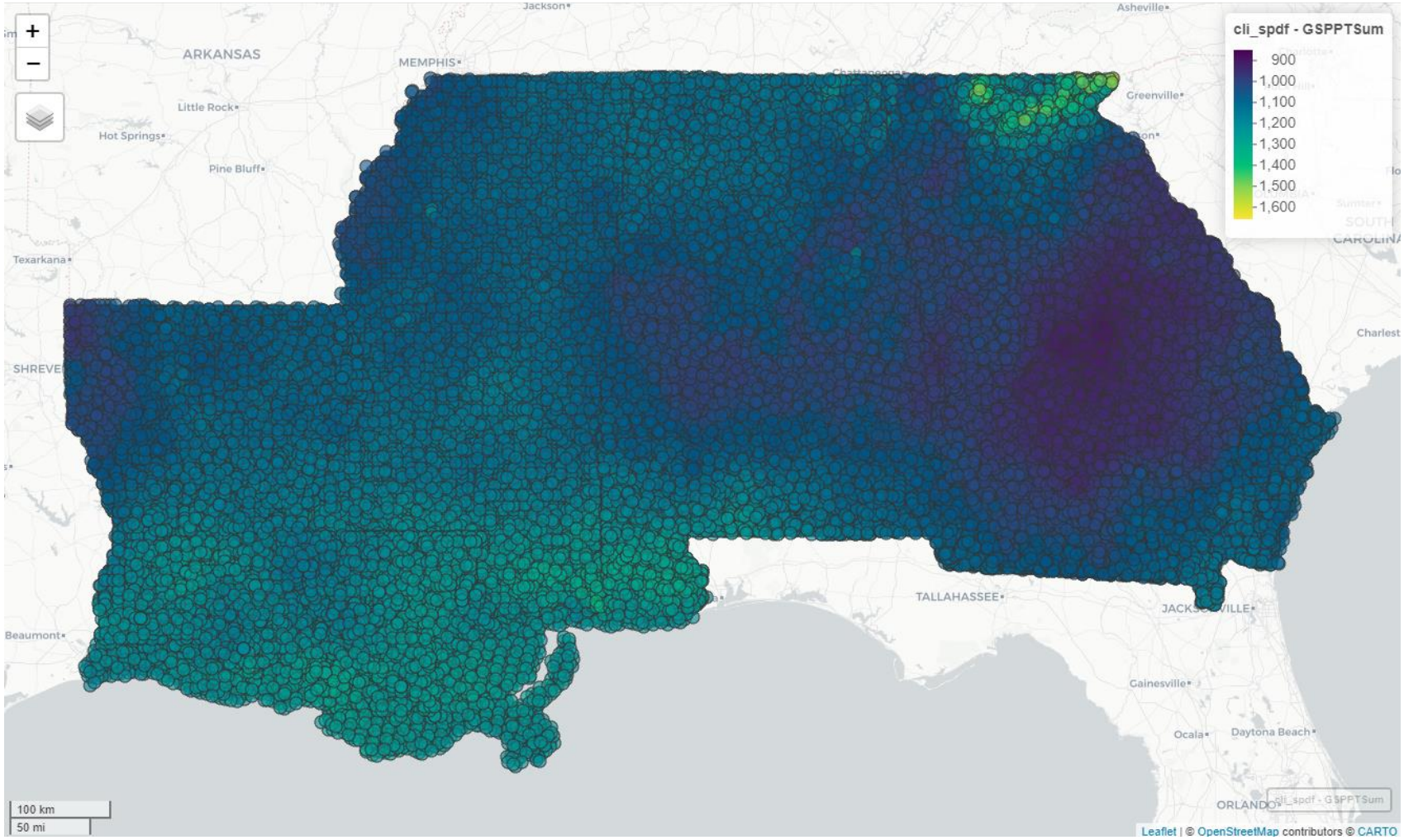

Figure 10 Total growing season precipitation by FIA plot across Alabama, Georgia, Louisiana, and Mississippi.

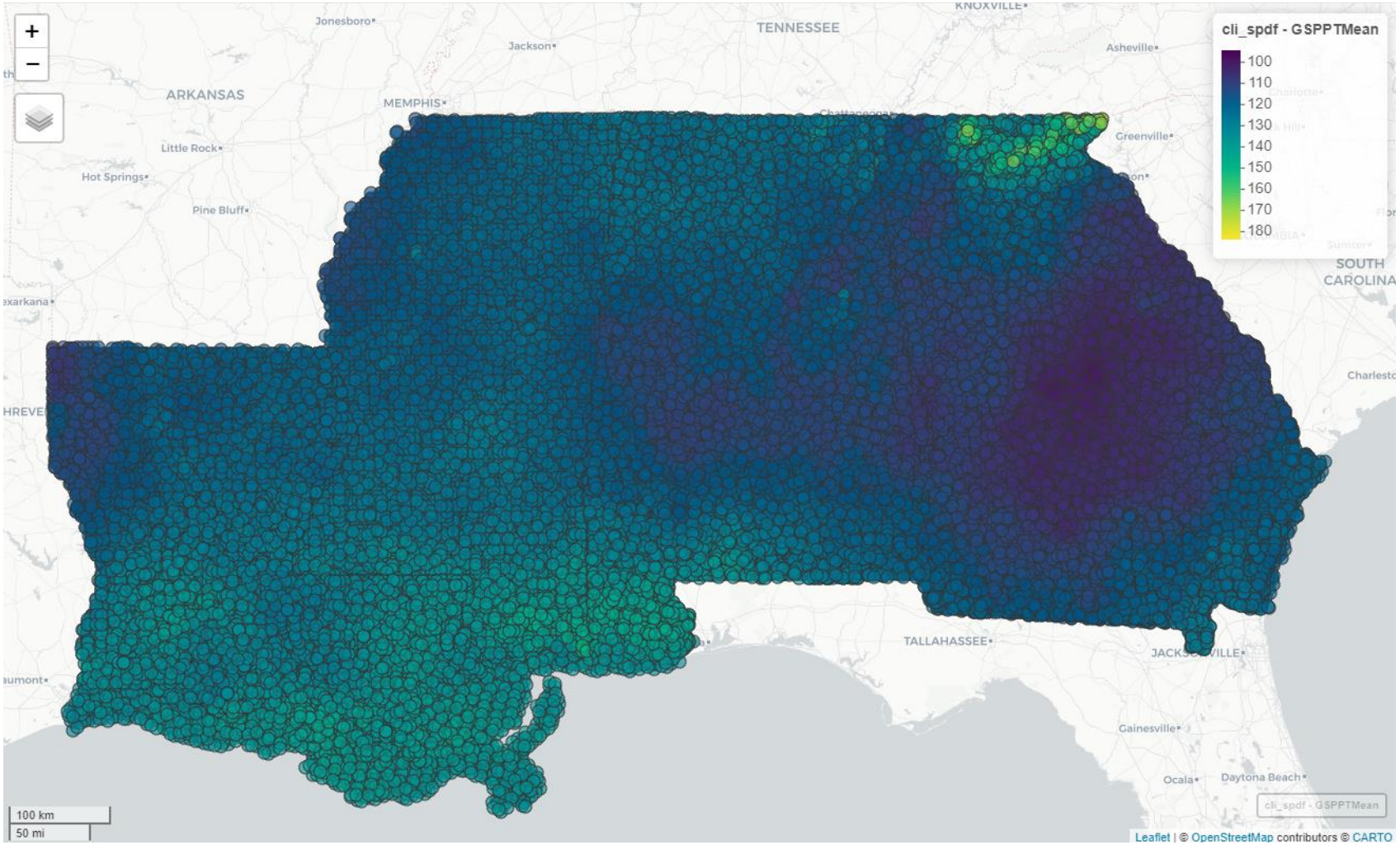

Figure 11 Mean monthly precipitation during the growing season by FIA plot across Alabama, Georgia, Louisiana, and Mississippi.

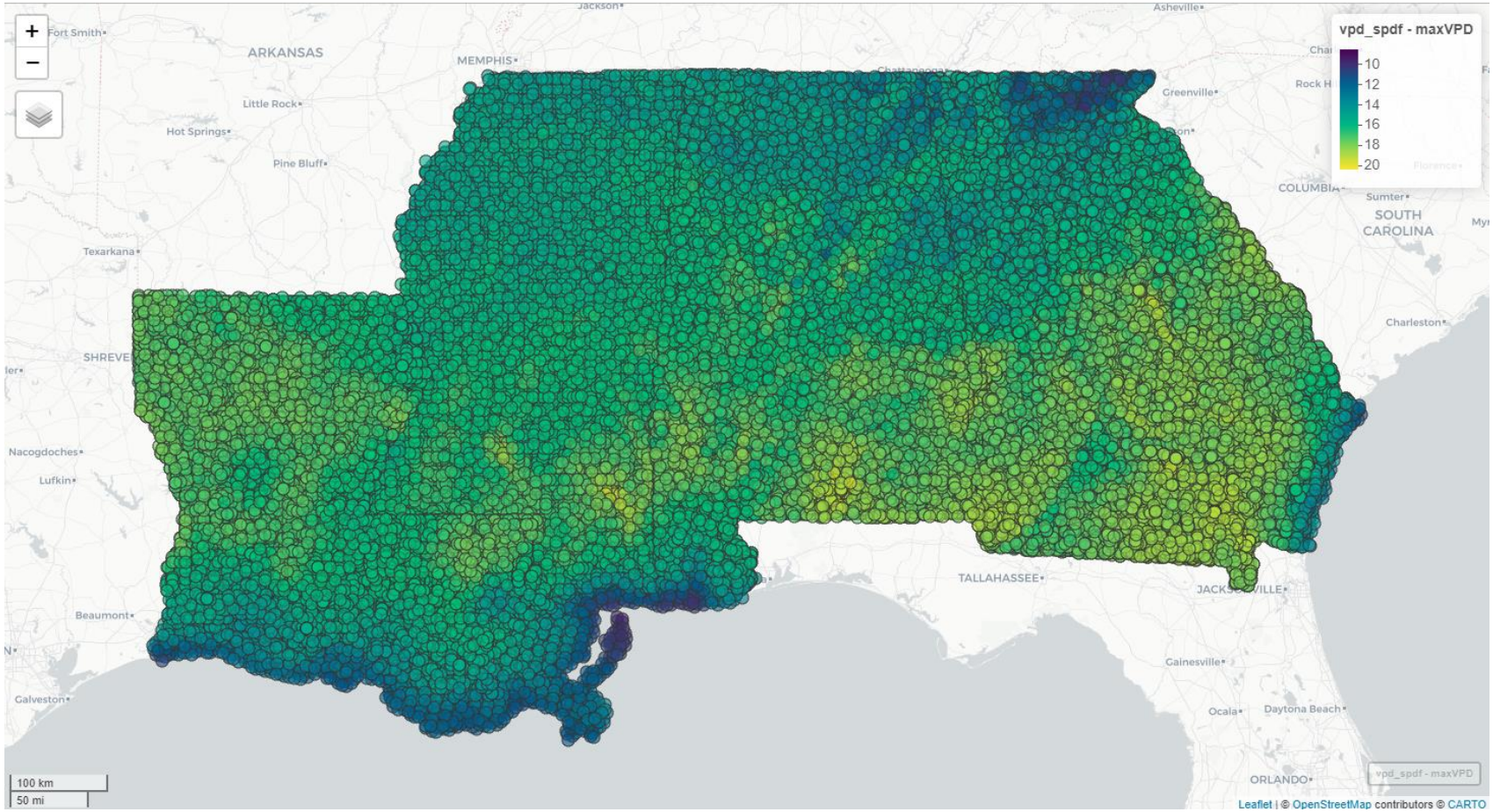

Figure 12 Average maximum vapor pressure deficit by FIA plot across Alabama, Georgia, Louisiana, and Mississippi.

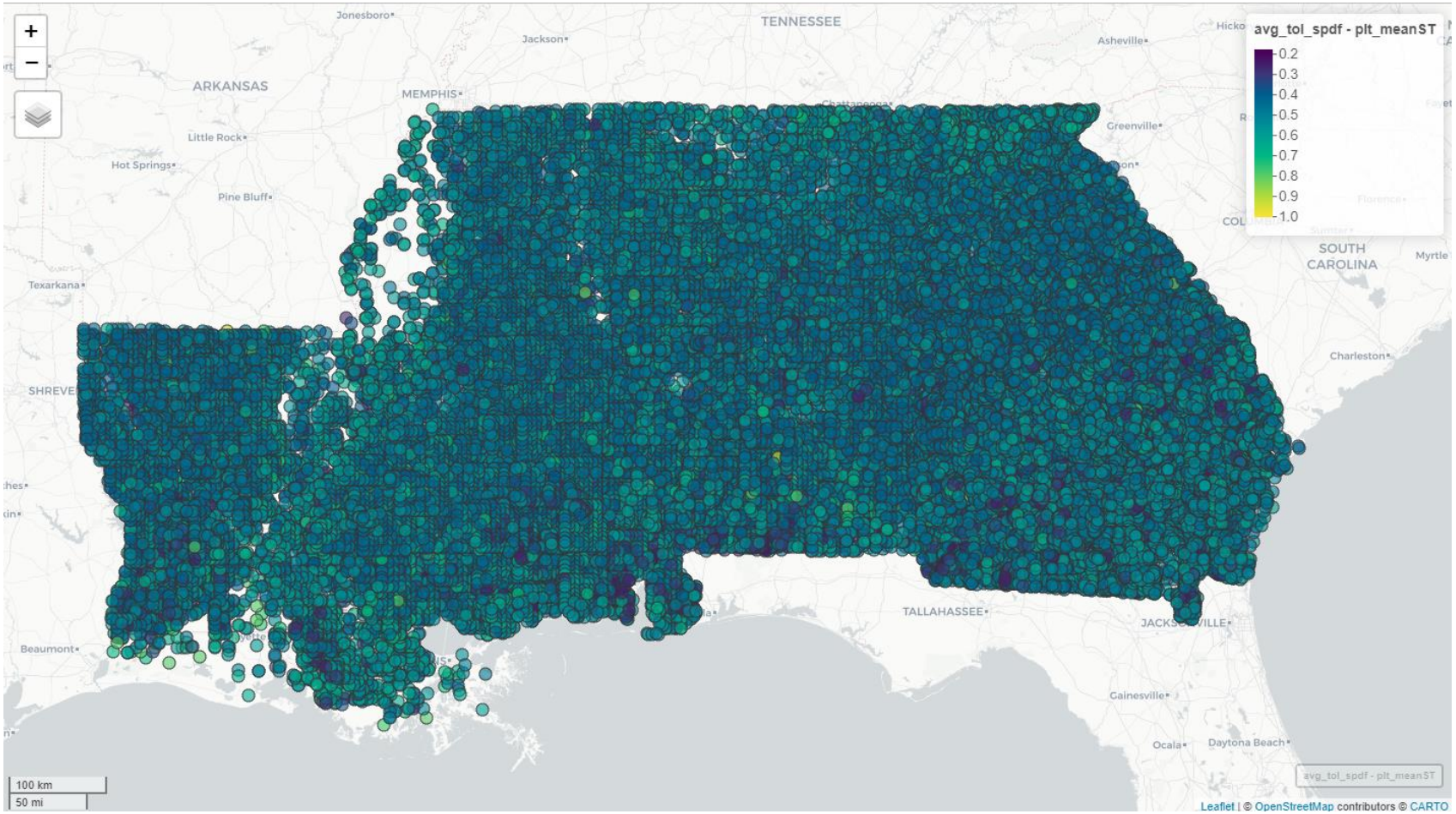

Figure 13 Average shade tolerance values by FIA plot across Alabama, Georgia, Louisiana, and Mississippi.

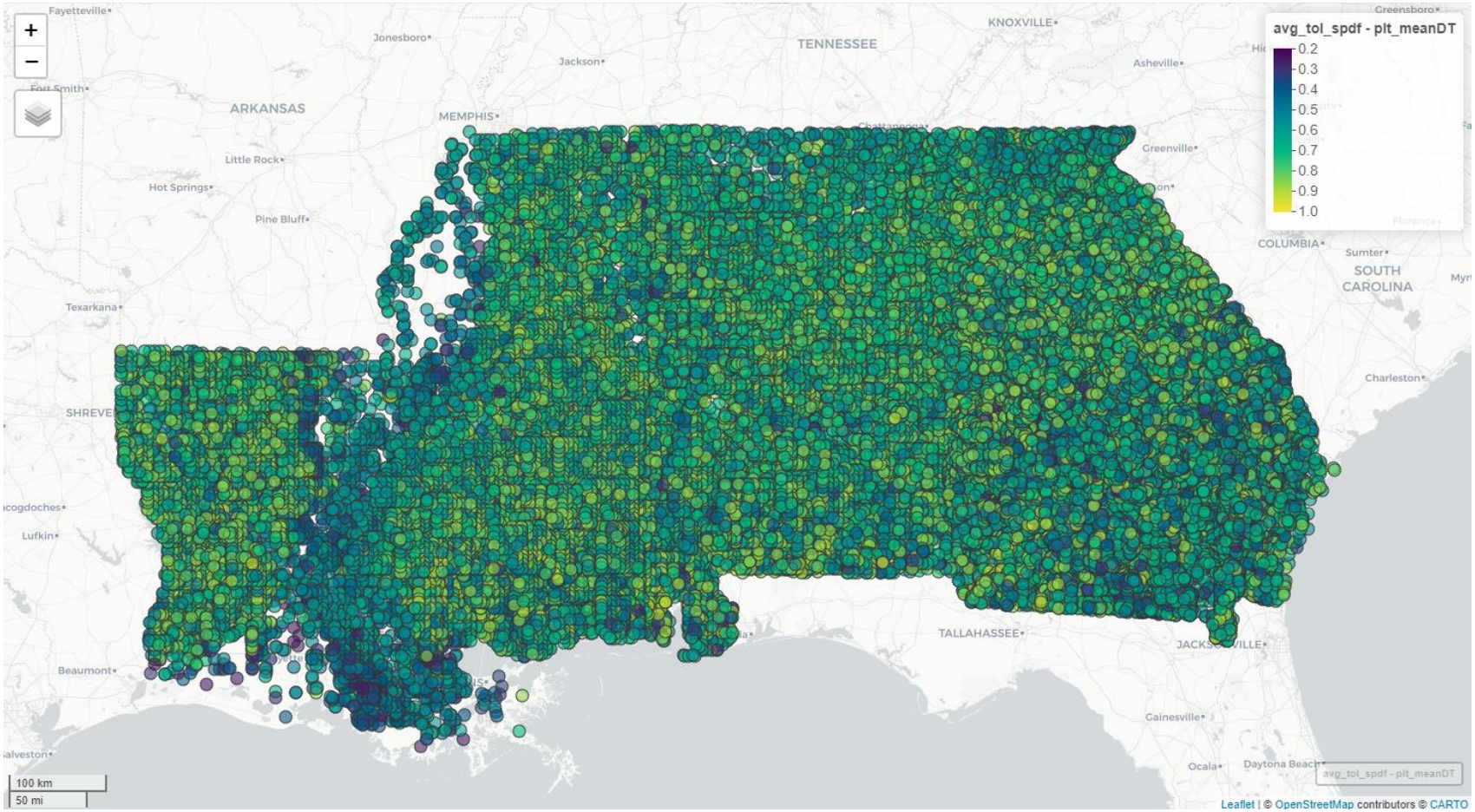

Figure 14 Average drought tolerance values by FIA plot across Alabama, Georgia, Louisiana, and Mississippi.

APPENDIX B

FUNCTIONAL TRAITS BY SPECIES

Table 5 Functional traits by species

Species FIA Code	Common Name	Scientific Name	Specific Gravity, 12% MC	Shade Tolerance	Drought Tolerance
16	Fraser fir	Abies fraseri	0.38	5.00	2.00
43	Atlantic white-cedar	Chamaecyparis thyoides	0.32	3.50	1.00
58	Pinchot juniper	Juniperus pinchotii	0.47	1.28	4.65
59	redberry juniper	Juniperus coahuilensis	0.47	1.28	4.65
61	Ashe juniper	Juniperus ashei	0.45	1.28	4.65
63	alligator juniper	Juniperus deppeana	0.51	2.00	5.00
66	Rocky Mountain juniper	Juniperus scopulorum	0.47	1.48	4.97
67	southern redcedar	Juniperus virginiana var. silicicola	0.42	1.28	4.65
68	eastern redcedar	Juniperus virginiana	0.47	1.28	4.65
69	oneseed juniper	Juniperus monosperma	0.47	2.00	5.00
70	larch spp.	Larix spp.	0.53	0.98	2.00
90	spruce spp.	Picea spp.	0.39	4.42	2.13
91	Norway spruce	Picea abies	0.39	4.45	1.75
106	common or two-needle pinyon	Pinus edulis	0.57	1.44	4.97
107	sand pine	Pinus clausa	0.48	2.21	2.25
110	shortleaf pine	Pinus echinata	0.51	1.86	4.00
111	slash pine	Pinus elliottii	0.59	2.65	3.50
115	spruce pine	Pinus glabra	0.44	4.50	2.50
121	longleaf pine	Pinus palustris	0.59	0.87	4.75
123	Table Mountain pine	Pinus pungens	0.49	1.90	4.00
125	red pine	Pinus resinosa	0.46	1.89	3.00
126	pitch pine	Pinus rigida	0.47	1.99	4.00
128	pond pine	Pinus serotina	0.51	1.47	3.00
129	eastern white pine	Pinus strobus	0.34	3.21	2.29
130	Scotch pine	Pinus sylvestris	0.47	1.67	4.34

Table 5 (Continued)

Species FIA Code	Common Name	Scientific Name	Specific Gravity, 12% MC	Shade Tolerance	Drought Tolerance
131	loblolly pine	Pinus taeda	0.51	1.99	4.50
132	Virginia pine	Pinus virginiana	0.48	1.99	4.00
136	Austrian pine	Pinus nigra	0.47	2.10	4.38
140	Mexican pinyon pine	Pinus cembroides	0.47	3.00	5.00
202	Douglas-fir	Pseudotsuga menziesii	0.48	2.78	2.62
221	baldcypress	Taxodium distichum	0.46	2.13	3.25
222	pondcypress	Taxodium ascendens	0.46	2.13	3.25
241	northern white-cedar	Thuja occidentalis	0.31	3.45	2.71
260	hemlock spp.	Tsuga spp.	0.41	4.83	1.00
261	eastern hemlock	Tsuga canadensis	0.40	4.83	1.00
262	Carolina hemlock	Tsuga caroliniana	0.41	4.83	1.00
310	maple spp.	Acer spp.	0.47	3.00	2.00
311	Florida maple	Acer barbatum	0.52	4.50	2.50
313	boxelder	Acer negundo	0.46	3.47	3.03
314	black maple	Acer nigrum	0.52	3.00	3.35
315	striped maple	Acer pensylvanicum	0.44	3.31	2.00
316	red maple	Acer rubrum	0.54	3.44	1.84
317	silver maple	Acer saccharinum	0.47	3.60	2.88
318	sugar maple	Acer saccharum	0.63	4.76	2.25
319	mountain maple	Acer spicatum	0.47	3.31	2.00
320	Norway maple	Acer platanoides	0.52	4.20	2.73
323	chalk maple	Acer leucoderme	0.47	4.76	2.25
330	buckeye, horsechestnut spp.	Aesculus spp.	0.33	3.64	2.33
331	Ohio buckeye	Aesculus glabra	0.33	3.49	2.88

Table 5 (Continued)

Species FIA Code	Common Name	Scientific Name	Specific Gravity, 12% MC	Shade Tolerance	Drought Tolerance
332	yellow buckeye	Aesculus flava	0.33	4.14	2.00
333	California buckeye	Aesculus californica	0.36	2.50	2.88
341	ailanthus	Ailanthus altissima	0.53	2.44	2.96
345	mimosa, silktree	Albizia julibrissin	0.58	1.17	4.47
350	alder spp.	Alnus spp.	0.41	2.71	2.22
355	European alder	Alnus glutinosa	0.41	2.71	2.22
356	serviceberry spp.	Amelanchier spp.	0.79	3.59	2.45
357	common serviceberry	Amelanchier arborea	0.66	4.33	2.38
363	Texas madrone	Arbutus xalapensis	0.65	3.32	3.83
367	pawpaw	Asimina triloba	0.58	3.95	2.00
370	birch spp.	Betula spp.	0.51	2.40	2.51
371	yellow birch	Betula alleghaniensis	0.55	3.17	3.00
372	sweet birch	Betula lenta	0.65	2.58	3.00
373	river birch	Betula nigra	0.56	1.45	1.53
375	paper birch	Betula papyrifera	0.55	1.54	2.02
379	gray birch	Betula populifolia	0.51	1.50	2.34
381	chittamwood, gum bumelia	Sideroxylon lanuginosum ssp. lanuginosum	0.58	2.64	2.91
391	American hornbeam, musclewood	Carpinus caroliniana	0.70	4.58	2.02
400	hickory spp.	Carya spp.	0.68	3.00	3.00
401	water hickory	Carya aquatica	0.62	2.95	2.00
402	bitternut hickory	Carya cordiformis	0.66	2.07	4.00
403	pignut hickory	Carya glabra	0.75	2.69	4.00
404	pecan	Carya illinoinensis	0.66	1.74	2.00
405	shellbark hickory	Carya laciniosa	0.69	4.42	2.00
406	nutmeg hickory	Carya myristiciformis	0.60	3.71	2.00

Table 5 (Continued)

Species FIA Code	Common Name	Scientific Name	Specific Gravity, 12% MC	Shade Tolerance	Drought Tolerance
407	shagbark hickory	Carya ovata	0.72	3.40	3.00
408	black hickory	Carya texana	0.68	2.69	4.00
409	mockernut hickory	Carya alba	0.72	2.20	3.00
410	sand hickory	Carya pallida	0.68	1.56	4.00
411	scrub hickory	Carya floridana	0.68	2.69	4.00
412	red hickory	Carya ovalis	0.68	2.69	4.00
413	southern shagbark hickory	Carya carolinae-septentrionalis	0.68	3.40	3.00
421	American chestnut	Castanea dentata	0.40	3.06	3.00
422	Allegheny chinkapin	Castanea pumila	0.43	2.50	4.00
423	Ozark chinkapin	Castanea pumila var. ozarkensis	0.40	2.50	4.00
424	Chinese chestnut	Castanea mollissima	0.43	1.67	2.63
450	catalpa spp.	Catalpa spp.	0.41	2.67	2.58
451	southern catalpa	Catalpa bignonioides	0.41	2.67	2.58
452	northern catalpa	Catalpa speciosa	0.38	2.33	4.22
460	hackberry spp.	Celtis spp.	0.49	2.68	3.80
461	sugarberry	Celtis laevigata	0.53	3.31	3.56
462	hackberry	Celtis occidentalis	0.53	3.17	3.85
463	netleaf hackberry	Celtis laevigata var. reticulata	0.49	3.31	3.56
471	eastern redbud	Cercis canadensis	0.58	3.00	4.05
481	yellowwood	Cladrastis kentukea	0.52	3.00	2.88
491	flowering dogwood	Cornus florida	0.73	4.87	2.92
500	hawthorn spp.	Crataegus spp.	0.58	1.97	3.90
501	cockspur hawthorn	Crataegus crus-galli	0.58	1.67	4.98
502	downy hawthorn	Crataegus mollis	0.52	1.97	3.90
510	eucalyptus spp.	Eucalyptus spp.	0.58	2.00	2.50

Table 5 (Continued)

Species FIA Code	Common Name	Scientific Name	Specific Gravity, 12% MC	Shade Tolerance	Drought Tolerance
513	grand eucalyptus	Eucalyptus grandis	0.58	2.00	2.50
521	common persimmon	Diospyros virginiana	0.74	4.21	1.50
522	Texas persimmon	Diospyros texana	0.74	4.21	1.50
531	American beech	Fagus grandifolia	0.64	4.75	1.50
540	ash spp.	Fraxinus spp.	0.51	2.78	2.60
541	white ash	Fraxinus americana	0.60	2.46	2.38
543	black ash	Fraxinus nigra	0.45	2.96	2.00
544	green ash	Fraxinus pennsylvanica	0.56	3.11	3.85
545	pumpkin ash	Fraxinus profunda	0.48	3.00	2.00
546	blue ash	Fraxinus quadrangulata	0.58	1.84	2.75
548	Carolina ash	Fraxinus caroliniana	0.51	3.50	2.00
549	Texas ash	Fraxinus texensis	0.55	2.46	2.38
550	honeylocust spp.	Gleditsia spp.	0.65	1.81	3.49
551	waterlocust	Gleditsia aquatica	0.65	2.00	2.00
552	honeylocust	Gleditsia triacanthos	0.65	1.61	4.98
555	loblolly-bay	Gordonia lasianthus	0.58	3.00	2.00
571	Kentucky coffeetree	Gymnocladus dioicus	0.60	2.50	3.69
580	silverbell spp.	Halesia spp.	0.42	3.11	2.00
581	Carolina silverbell	Halesia carolina	0.42	3.11	2.00
582	two-wing silverbell	Halesia diptera	0.45	3.11	2.00
591	American holly	Ilex opaca	0.57	4.28	2.92
600	walnut spp.	Juglans spp.	0.47	1.91	2.38
601	butternut	Juglans cinerea	0.36	1.88	2.38
602	black walnut	Juglans nigra	0.55	1.93	2.38
605	Texas walnut	Juglans microcarpa	0.47	1.35	4.95

Table 5 (Continued)

Species FIA Code	Common Name	Scientific Name	Specific Gravity, 12% MC	Shade Tolerance	Drought Tolerance
606	Arizona walnut	Juglans major	0.47	1.35	4.95
611	sweetgum	Liquidambar styraciflua	0.52	1.59	2.92
621	yellow-poplar	Liriodendron tulipifera	0.42	2.07	2.60
641	Osage-orange	Maclura pomifera	0.85	1.45	4.22
650	magnolia spp.	Magnolia spp.	0.47	3.25	1.81
651	cucumbertree	Magnolia acuminata	0.48	3.03	1.27
652	southern magnolia	Magnolia grandiflora	0.50	4.50	2.88
653	sweetbay	Magnolia virginiana	0.46	3.00	1.50
654	bigleaf magnolia	Magnolia macrophylla	0.47	3.11	1.00
655	mountain or Fraser magnolia	Magnolia fraseri	0.40	3.06	2.00
658	umbrella magnolia	Magnolia tripetala	0.43	3.06	2.00
660	apple spp.	Malus spp.	0.67	1.50	2.50
661	Oregon crab apple	Malus fusca	0.61	1.50	2.50
662	southern crab apple	Malus angustifolia	0.67	1.50	2.50
663	sweet crab apple	Malus coronaria	0.67	1.50	2.50
664	prairie crab apple	Malus ioensis	0.67	1.50	2.50
680	mulberry spp.	Morus spp.	0.52	1.85	2.88
681	white mulberry	Morus alba	0.52	1.35	2.88
682	red mulberry	Morus rubra	0.58	2.34	2.88
683	Texas mulberry	Morus microphylla	0.58	2.34	2.88
691	water tupelo	Nyssa aquatica	0.50	3.47	1.00
692	Ogeechee tupelo	Nyssa ogeche	0.46	4.00	2.00
693	blackgum	Nyssa sylvatica	0.50	3.52	2.00
694	swamp tupelo	Nyssa biflora	0.50	2.00	1.00
701	eastern hophornbeam	Ostrya virginiana	0.70	4.58	3.25

Table 5 (Continued)

Species FIA Code	Common Name	Scientific Name	Specific Gravity, 12% MC	Shade Tolerance	Drought Tolerance
711	sourwood	Oxydendrum arboreum	0.55	2.70	3.00
712	paulownia, empress-tree	Paulownia tomentosa	0.58	2.00	3.00
721	redbay	Persea borbonia	0.58	4.00	2.00
722	water-elm, planertree	Planera aquatica	0.58	4.00	2.00
731	American sycamore	Platanus occidentalis	0.49	2.86	2.25
740	cottonwood and poplar spp.	Populus spp.	0.39	1.00	3.00
741	balsam poplar	Populus balsamifera	0.34	1.27	1.77
742	eastern cottonwood	Populus deltoides	0.40	1.76	1.57
743	bigtooth aspen	Populus grandidentata	0.39	1.21	2.50
744	swamp cottonwood	Populus heterophylla	0.39	1.24	2.00
745	plains cottonwood	Populus deltoides ssp. monilifera	0.39	1.76	1.57
746	quaking aspen	Populus tremuloides	0.38	1.21	1.77
752	silver poplar	Populus alba	0.35	2.30	2.67
756	honey mesquite	Prosopis glandulosa	0.82	1.17	4.95
758	screwbean mesquite	Prosopis pubescens	0.82	1.17	4.95
760	cherry and plum spp.	Prunus spp.	0.50	2.21	2.78
761	pin cherry	Prunus pensylvanica	0.47	1.00	3.00
762	black cherry	Prunus serotina	0.50	2.46	3.02
763	chokecherry	Prunus virginiana	0.50	2.59	2.88
766	American plum	Prunus americana	0.50	2.21	2.78
771	sweet cherry, domesticated	Prunus avium	0.50	3.33	2.66
800	oak spp.	Quercus spp.	0.66	2.33	3.28
802	white oak	Quercus alba	0.68	2.85	3.56
804	swamp white oak	Quercus bicolor	0.72	2.98	3.35
806	scarlet oak	Quercus coccinea	0.67	2.07	4.00

Table 5 (Continued)

Species FIA Code	Common Name	Scientific Name	Specific Gravity, 12% MC	Shade Tolerance	Drought Tolerance
807	blue oak	Quercus douglasii	0.59	2.00	5.00
808	Durand oak	Quercus sinuata var. sinuata	0.66	2.85	3.56
809	northern pin oak	Quercus ellipsoidalis	0.66	2.49	2.38
810	Emory oak	Quercus emoryi	0.66	3.00	4.00
812	southern red oak	Quercus falcata	0.59	2.50	5.00
813	cherrybark oak	Quercus pagoda	0.69	2.24	2.50
816	scrub oak	Quercus ilicifolia	0.66	2.50	3.63
817	shingle oak	Quercus imbricaria	0.59	2.09	3.85
819	turkey oak	Quercus laevis	0.66	2.00	5.00
820	laurel oak	Quercus laurifolia	0.63	3.34	3.00
822	overcup oak	Quercus lyrata	0.63	2.97	1.00
823	bur oak	Quercus macrocarpa	0.64	2.71	3.85
824	blackjack oak	Quercus marilandica	0.66	3.00	4.00
825	swamp chestnut oak	Quercus michauxii	0.67	2.85	3.50
826	chinkapin oak	Quercus muehlenbergii	0.66	2.22	4.97
827	water oak	Quercus nigra	0.63	2.24	3.00
828	Texas red oak	Quercus texana	0.66	2.49	2.38
830	pin oak	Quercus palustris	0.63	2.49	2.38
831	willow oak	Quercus phellos	0.69	2.00	1.00
832	chestnut oak	Quercus prinus	0.66	2.85	3.50
833	northern red oak	Quercus rubra	0.63	2.75	2.88
834	Shumard oak	Quercus shumardii	0.66	2.35	4.65
835	post oak	Quercus stellata	0.67	2.16	4.50
836	Delta post oak	Quercus similis	0.66	2.16	4.50
837	black oak	Quercus velutina	0.61	2.72	3.00

Table 5 (Continued)

Species FIA Code	Common Name	Scientific Name	Specific Gravity, 12% MC	Shade Tolerance	Drought Tolerance
838	live oak	Quercus virginiana	0.88	2.24	4.50
840	dwarf post oak	Quercus margarettiae	0.66	2.16	4.50
841	dwarf live oak	Quercus minima	0.59	2.24	4.50
842	bluejack oak	Quercus incana	0.66	2.50	4.50
844	Oglethorpe oak	Quercus oglethorpensis	0.59	2.85	3.56
853	pond-apple	Annona glabra	0.58	2.64	2.91
854	gumbo limbo	Bursera simaruba	0.58	2.64	2.91
855	sheoak spp.	Casuarina spp.	0.58	2.64	2.91
857	belah	Casuarina lepidophloia	0.58	2.64	2.91
858	camphortree	Cinnamomum camphora	0.52	3.50	2.75
860	citrus spp.	Citrus spp.	0.58	2.00	3.00
863	tietongue, pigeon-plum	Coccoloba diversifolia	0.58	2.64	2.91
876	Florida strangler fig	Ficus aurea	0.58	2.64	2.91
882	beeftree, longleaf blolly	Guapira discolor	0.58	2.64	2.91
886	Florida poisontree	Metopium toxiferum	0.58	2.64	2.91
887	fishpoison tree	Piscidia piscipula	0.58	2.64	2.91
896	Java plum	Syzygium cumini	0.58	2.64	2.91
897	tamarind	Tamarindus indica	0.58	2.64	2.91
901	black locust	Robinia pseudoacacia	0.69	1.72	4.11
909	royal palm spp.	Roystonea spp.	0.58	2.00	4.00
912	cabbage palmetto	Sabal palmetto	0.52	2.00	4.00
913	key thatch palm	Thrinax morrisii	0.58	2.00	4.00
915	other palms	Family Arecaceae not listed above	0.58	2.00	4.00
920	willow spp.	Salix spp.	0.39	1.00	1.00
921	peachleaf willow	Salix amygdaloides	0.39	1.17	1.77

Table 5 (Continued)

Species FIA Code	Common Name	Scientific Name	Specific Gravity, 12% MC	Shade Tolerance	Drought Tolerance
922	black willow	Salix nigra	0.39	1.34	1.77
925	coastal plain willow	Salix caroliniana	0.36	1.50	2.00
927	white willow	Salix alba	0.39	1.99	2.00
929	weeping willow	Salix sepulcralis	0.39	1.35	1.77
931	sassafras	Sassafras albidum	0.46	1.68	5.00
935	American mountain-ash	Sorbus americana	0.58	2.59	1.77
940	West Indian mahogany	Swietenia mahagoni	0.58	3.00	4.00
950	basswood spp.	Tilia spp.	0.32	3.67	2.29
951	American basswood	Tilia americana	0.37	3.98	2.88
952	white basswood	Tilia americana var. heterophylla	0.32	3.77	2.00
953	Carolina basswood	Tilia americana var. caroliniana	0.37	3.98	2.88
970	elm spp.	Ulmus spp.	0.54	3.16	3.14
971	winged elm	Ulmus alata	0.66	3.03	3.50
972	American elm	Ulmus americana	0.50	3.14	2.92
973	cedar elm	Ulmus crassifolia	0.59	3.00	3.00
974	Siberian elm	Ulmus pumila	0.54	2.50	3.35
975	slippery elm	Ulmus rubra	0.53	3.31	3.00
976	September elm	Ulmus serotina	0.54	3.22	2.00
977	rock elm	Ulmus thomasii	0.57	3.22	2.00
986	black-mangrove	Avicennia germinans	0.58	2.64	2.91
987	buttonwood-mangrove	Conocarpus erectus	0.58	2.64	2.91
988	white-mangrove	Laguncularia racemosa	0.58	2.64	2.91
989	American mangrove	Rhizophora mangle	0.58	2.64	2.91
992	melaleuca	Melaleuca quinquenervia	0.58	2.00	2.00
993	chinaberry	Melia azedarach	0.58	3.00	2.85

Table 5 (Continued)

Species FIA Code	Common Name	Scientific Name	Specific Gravity, 12% MC	Shade Tolerance	Drought Tolerance
994	Chinese tallowtree	Triadica sebifera	0.58	4.00	1.00
995	tungoil tree	Vernicia fordii	0.58	1.00	5.00
996	smoketree	Cotinus obovatus	0.58	3.00	3.96
997	Russian-olive	Elaeagnus angustifolia	0.58	1.35	4.47
6511	swamp bay	Persea palustris	0.58	4.00	2.00
6696	cherry laurel	Prunus laurocerasus	0.50	4.11	2.21
6791	myrtle oak	Quercus myrtifolia	0.80	1.50	4.50
6799	bastard oak	Quercus sinuata	0.66	2.85	3.56
7328	mountain silverbell	Halesia tetraptera	0.45	3.11	2.00
7577	Japanese privet	Ligustrum japonicum	0.58	3.50	2.50
7578	glossy privet	Ligustrum lucidum	0.58	3.50	2.50
8345	Carolina laurelcherry	Prunus caroliniana	0.50	1.50	3.00
8420	pear spp.	Pyrus spp.	0.69	1.35	4.47
8421	Callery pear	Pyrus calleryana	0.69	1.35	4.47
8427	sawtooth oak	Quercus acutissima	0.78	2.30	3.99
8441	sand live oak	Quercus geminata	0.66	2.33	3.28
8449	Darlington oak	Quercus hemisphaerica	0.66	2.50	3.63
8487	bastard oak	Quercus sinuata var. breviloba	0.66	2.85	3.56
8514	Lacey oak	Quercus laceyi	0.66	2.50	3.63